NOTE TO USERS

A study of atmospheric properties and their impact on the use of the Nocturnal Boundary Layer budget technique for trace gas measurement

Nathalie Mathieu

Department of Natural Resources Sciences
McGill University, Montréal

August, 2004

A thesis submitted to McGill University in partial fulfillment of the requirements of the degree of Master of Science.

Your file Votre référence
ISBN: 0-494-12502-0
Our file Notre référence
ISBN: 0-494-12502-0

Suggested short title:

Atmospheric impact on the Nocturnal Boundary Layer technique

Nathalie Mathieu

Contents

Figures

Tables

Preface

Candidates have the option of including, as part of the thesis, the text of one or more papers submitted, or to be submitted, for publication, or the clearly-duplicated text (not the reprints) of one or more published papers. These texts must be bound together as an integral part of the thesis.

Choosing this option implies that connecting texts that provide logical bridges preceding and following each manuscript are mandatory. The thesis must be more than a collection of manuscripts. All components must be integrated into a cohesive unit with a logical progression from one chapter to the next.

The thesis must conform to all other requirements of the "Guidelines for Thesis Preparation" in addition to the manuscripts. This thesis must include: a table of contents, an abstract in English and French, an introduction that clearly states the rationale and objectives of the study, a review of literature, a final conclusion and summary, and a thorough bibliography or reference list.

Additional material must be provided where appropriate (e.g., in appendices) in sufficient detail to allow a clear and precise judgement to be made of the importance and originality of the research reported in the thesis.

In the case of manuscripts co-authored, the candidate is required to make an explicit statement in the thesis as to who contributed to such work and to what extent. This statement should appear in a single section entitled "Contributions of Authors" as a preface to the thesis.

This thesis consists of three manuscripts.

Observations of Gas Accumulation under a Low-Level Jet

Nathalie Mathieu, Ian B. Strachan, Monique Y. Leclerc and Anandakumar Karipot

This manuscript is the original work of Nathalie Mathieu, with the following exceptions. Dr. Ian B. Strachan supervised the research, provided expert advice, financial assistance and contributed in the editing process. Dr. Monique Y. Leclerc provided expert advice and made possible the use of the mini-SODAR. Dr. Karipot provided expert advice.

Continuous Vertical motion under the Nocturnal Boundary Layer and Impact of Intermittent Turbulence

Nathalie Mathieu, Ian B. Strachan, Monique Y. Leclerc and Volker Thiermann

This manuscript is the original work of Nathalie Mathieu, with the following exceptions. Dr. Ian B. Strachan supervised the research, provided expert advice, financial assistance and contributed in the editing process. Dr Monique Y. Leclerc provided expert advice and made possible the use of the mini-SODAR. Dr. Volker Thiermann (Scintec Inc.) provided input on technical questions concerning the mini-SODAR.

Breakdown of the NBL and its Impact on the NBL Technique

This manuscript is the original work of Nathalie Mathieu. Dr. Ian B. Strachan provided supervision, financial support and contributed in the editing process.

Acknowledgements

I would like to express my gratitude to my supervisor Dr. Ian B. Strachan for his continuous support, generosity, motivation and advice throughout the different processes leading to this Master thesis. I also whish to thank Dr. Monique Y. Leclerc for her expert advice and making possible the uses of the mini-SODAR; Dr Elisabeth Pattey for providing recommendations regarding the NBL technique and different measurement components during the field campaigns, Dr. Anand Karipot, Dr. Volker Thierman, Dr. Peter Bartello and Eva Monteiro for their advices.

I wish to thank my lab partner, Laura Wittebol, who inspired me by her hard work, the long talks we had and her generosity in the help she provided.

This research would have never been possible without all research assistants working for the NBL team: Melissa Valiquette, Diane Poon, YaoHua Law, Mélissa Hairabedian, Clare Salustro, Lynda Blackburn, Matthew Hinther and all the professionals: Dave Dow, Christophe Forget and Jesus Mata for help with summer field work, lab analysis, and data processing at various stages of the project. The contribution of the McGill staff was invaluable on so many levels; I especially want to thank Ornella Cavaliere, Marie Kubecki and Arnold.

I also thank my parents, sisters, friends and my life partner, Christophe Forget, for their continuing support and my grandmother for her wise guidance. You're all a part of who I've become and what I've accomplished.

Abstract

While most micrometeorological measurement techniques are only suitable for windy conditions, the Nocturnal Boundary Layer Technique can be used to measure trace gas flux during calm, clear nights as the nighttime stability enables gas emitted at the ground to accumulate. The difference between two measurements over the whole depth of this layer is believed to integrate emissions from a large area representative of, in this study, an agricultural farm. A tethersonde and infrared gas analyzer attached to a blimp carrying a bag sampling system monitored atmospheric variables for each ascent during two summer field campaigns. A mini-SODAR was installed in the field to obtain the wind flowfield. Strong accumulation was observed under low level jets suggesting that this feature acts as a good lid for trace gases. An average background vertical motion different from zero seemed to have more influence on gas propagation than did intermittent turbulence. On at least one night, a density current created by the nearby St-Lawrence River was observed to influence measurements.

Résumé

Alors que la majorité des techniques de mesures micrométéorologiques ne sont valable qu'en conditions turbulentes, la technique de couche-limite nocturne peut être utilisée pour mesurer les flux de gaz présents à l'état de trace pendant les nuits claires et calmes puisque la stabilité nocturne permet l'accumualtion des gaz emis à la surface. Il est supposé que la différence entre deux mesures prises sur toute la hauteur de la couche-limite intègre les émissions d'une grande surface représentant, dans notre cas, une ferme agricole. Une sonde et un analyseur de gaz à infrarouge attachés à un ballon dirigeable transportant un système de collecte de gaz, ont récupérés les variables atmosphériques lors de deux étés de cueillette de données sur le terrain. De plus, un mini-SODAR prenait des mesures de vents dans les champs. La grande capacité d'accumulation en dessous du courant jet de basse altitude suggère que celui-ci est très imperméable aux gaz. Un mouvement moyen différent de zéro semble avoir plus d'influence sur la propagations des gaz que la turbulence intermittente. Finalement, on a observé l'impact d'un courant atmosphérique créé par le fleuve St-Laurent dans les mesures de gaz.

Chapter 1: Introduction

Uncertainties surrounding our best estimates of greenhouse gas (GHG) emissions represent one of the most pressing issues not only in terms of assessment of the severity of climate change, but also in terms of the development of policy, protocols and regulations controlling the amount of greenhouse gases emitted into the atmosphere. Yet, uncertainties in agricultural GHG emissions remain high and are largely attributable to the necessary extrapolations of point measurements through time and space. One source of uncertainty lies with the different regime that exists during the nighttime period in comparison with the well-studied daytime regime.

Direct measurements of GHG's are made using a variety of techniques with micrometeorological methods receiving favour because of their ability to integrate over space continuously in the time domain. While most micrometeorological measurement techniques are only suitable during daytime or windy conditions, the Nocturnal Boundary Layer (NBL) technique, first introduced by Denmead (1996), can be used to measure trace gas flux during calm, clear nights as the nighttime stability enables gas emitted at the ground to accumulate. Thus, this technique may provide the ability to improve our estimates of GHG emissions by filling the existing void in calm nighttime conditions. Additionally, the NBL technique is believed to integrate emissions from larger areas representative of, in our case, an agricultural farm.

There is clearly a need to assess the NBL technique in particular and study the nighttime regime in general. The fluxes of GHG derived using the NBL technique must be placed in the proper context with acknowledgment of the different atmospheric features and events unique to the NBL which may have an impact on the gas

accumulation. The NBL technique relies on a secure knowledge of the height of the nocturnal stable layer, however, such information often proves elusive. While the NBL technique is generally thought to be robust and has been used previously to compare model output (e.g., Griffith, 2002), it has never been fully investigated. It is therefore currently difficult to associate a level of confidence in any computed flux estimates using the technique.

This study therefore had several objectives in terms of the use of the NBL budget technique:

1. To better define the height of the NBL through the combined use of mini-SODAR and tethered meteorological towers;
2. To explore the role of atmospheric features such as intermittency in determining the suitability of nights; and
3. To document sources of error and atmospheric events that may lead to data misinterpretation and errors in flux calculation.

1.1 Greenhouse gases

Greenhouse gases naturally absorb the longwave radiation emitted from Earth's surface in selective wavelengths and a portion of the radiation emitted by these atmospheric constituents returns to the Earth. When the concentration of these selective greenhouse gas absorbers is increased through human activities, the natural atmospheric greenhouse effect is enhanced (Please note that the term greenhouse gases within this document will henceforth be used to specifically designate anthropogenic greenhouse gases). The scientific community now accepts that the increased levels of greenhouse gases are causing a global warming effect (Chatterjee and Huq, 2002). This idea was first introduced by Arrhenius in 1896. An analysis of temperature records shows that the Earth has warmed an average of 0.5°C over the past 100 years (Environment Canada). It is also believed that this change could be responsible for an increase in the occurrence and intensity of severe weather events. The Kyoto protocol, a play for the reduction in greenhouse gases emission was established in 1997 between the Parties to the United Nations Framework Convention on Climate Change (UNFCCC, 1997; Tuhkanen *et al.*, 1999). The target is to reduce emission to a prescribed level for carbon dioxide, methane, and nitrous oxide (CO_2, CH_4, N_2O) and some fluorinated gases, i.e. HFCs, PFCs and SF_6 (UNFCCC, 1997) by 2010, to 6% below 1990 values (Kulshreshtha *et al.*, 2000). At present, there appear to be no easy solutions, and more will need to be done before any technological innovations can begin to solve this global issue (Hoffert *et al.*, 2002).

A number of research areas stem from the increasing interest in studying greenhouse gases, but few of them focus on the improvement of measurement techniques and the reduction in uncertainty surrounding measurements. Further, the interest has been

mainly on carbon dioxide; arguably the most important anthropogenic greenhouse gas, but not the one with the greatest warming potential (Tuhkanen *et al.*, 1999). Expressed in CO_2 equivalent units, N_2O and methane CH_4 have 310 and 21 times, respectively, the warming potential of CO_2 (Olsen *et al.*, 2003). However, the current lack of knowledge and inability to measure those gases in all circumstances lead to uncertainties of 40% and 30% of our best estimates of N_2O and CH_4, respectively compared to 4% for CO_2 (Olsen *et al.*, 2003). Certainly, future regulations implemented to attain the goals of international protocols need a stronger basis on the actual levels of emissions to be effective (Alcamo and Swart, 1998).

N_2O and CH_4 are the two principal greenhouse gases from the agriculture sector (approximated at 60%, 40%, respectively) and represent 8.3% of the total GHG emissions in Canada (Olsen *et al.*, 2003). Improved estimates of the emissions of these two gases are essential for reporting to the Canadian inventory as part of our commitment to international treaties such as the Kyoto protocol. The numbers that are currently available are largely estimated from models based on a select few measurements, which are themselves often made at small spatial scales at a small number of different locations (Olsen *et al*, 2003). Further complicating matters is the fact that nighttime measurements are less reliable. Experimentalists will typically use modeled values exclusively to replace missing or invalid nighttime flux values (Foken and Leclerc, 2004) resulting in the potential for large uncertainties (Moncrieff *et al.*, 1996). While modeling is clearly an essential component of estimating emissions, the model's results themselves have to be confirmed by more measurements. This will require the development of techniques that are valid at night and are representative of larger spatial scales.

1.2 Trace gas measurement techniques

The goal of obtaining more precise measurements of greenhouse gas emissions is harder to achieve than it seems. All measurement techniques have inherent weaknesses but it is worse when the causes of these failures for some of the techniques are still unknown. Efforts are currently underway to obtain a better sense of the uncertainties involved in using flux measurement techniques. Current techniques include chambers, tower-based micrometeorology, mass balance, convective boundary layer budgeting and nocturnal boundary layer budgeting (Denmead *et al.*, 1999).

In general, the flux of a trace gas can be found from:

$$F_S = \overline{w's'} + \int_0^z (\partial s/\partial t) dz + A \qquad (1)$$

where the first term represents the turbulent exchange written as a covariance between vertical wind speed w and gas concentration s. The second term represents the concentration change with time between the surface and a measurement height z, and the final term represents advection.

1.2.1 Eddy covariance

There are good reasons why eddy covariance (or eddy correlation) is the most widely used technique for surface trace gas flux measurement. It provides nearly continuous direct measurements of trace gas exchange between the surface and the atmosphere. Equation (1), itself a simplification, is further reduced to

$$F_S = \overline{w'\rho_s'} \qquad (2)$$

where w is the vertical wind speed (ms^{-1}), ρ (gcm^{-3}) is the trace gas density and storage and advection are assumed negligible. This assumption is valid in most studied agroecosystems where the canopy airspace of the short crops is relatively small and studied fields are relatively flat. The three dimensional wind components are resolved so that mean vertical windspeed is zero (Fowler *et al.*, 1995). Typically, a three-dimensional sonic anemometer with a response time of 10 Hz and a flux averaging period of 30-minutes will capture the spectrum of turbulent eddies (Fowler *et al.*, 1995). This technique is especially suitable for the measurement of CO_2 when used in combination with a fast-response infra red gas analyzer (IRGA) and has been adopted by the scientific community as the primary system for its calculation.

The requirements for the use of the eddy covariance micrometeorological technique include a homogeneous flat terrain, steady-state environmental conditions and that the underlying vegetation extends upwind for an extended distance (Baldocchi, 2003). The terrain can be chosen, but meteorological conditions cannot be set. Since the presence of a turbulent air stream is one of the basic requirements of eddy covariance, when turbulence is diminished, intermittent or absent (as in stable atmospheres), errors will result that get magnified once integrated over time to obtain daily and annual estimates (Baldocchi, 2003; Moncrieff *et al.*, 1996). As stable atmospheres are a common nighttime condition, an underestimation of CO_2 fluxes during nighttime periods is a reality that must be faced. This has led to the development of screening criteria for eddy covariance data. Recently, Pattey *et al.* (2002) set a limitation for agriculture at a friction velocity threshold of 0.075 to 0.1 ms^{-1} where the turbulence was strong enough to give reasonable flux estimate. During periods that do not meet screening criteria, it is common

to replace missing data with averages taken during the windy conditions, but this method may lead to underestimation of the true values (Pattey *et al.*, 2002).

1.2.2 Flux gradient technique

While CO_2 is commonly measured using eddy covariance, the other two dominant agricultural greenhouse gases (N_2O and CH_4) are currently measured using the flux gradient method. This well-established technique is defined by

$$F_s = -K\frac{\partial \rho_s}{\partial z} \qquad (3)$$

where F_S is the trace gas flux (ng m^{-2} s^{-1} for N_2O), K is the eddy diffusivity (m^2 s^{-1}), and $\partial \rho_s/\partial z$ is the concentration gradient of the trace gas (Businger, 1986). Like eddy covariance, an averaging period of 30 minutes is typically chosen to estimate the fluxes. Gas concentrations of N_2O and CH_4 are resolved using a tunable dual laser tunable gas analyzer (TDL-TGA) (Edwards *et al.*, 1994; 2003; Wagner-Riddle *et al*, 1996a; 1996b) while the eddy diffusivity is calculated with the data from either a sonic anemometer or a wind profile with at least four anemometers. This technique has the same turbulence dependence as eddy covariance because K is ill-defined during stable, non-turbulent periods.

1.2.3 Chambers

Unlike micrometeorological techniques, chambers measure gas emissions by trapping the emitted gas within a fixed volume. Samples are then either extracted at a regular time interval to be analyzed (e.g. gas chromatograph) or are dynamically measured (e.g. using portable CO_2 analysers in dynamic closed chambers) (Rochette *et al.*, 1997). This technique is widely used, but is really appropriate for small-scale experimental studies (Rochette *et al.*, 1997). The use of chambers, assumes to some degree, homogeneity in the emission between sampling times and therefore depends on the number of samples and their temporal spacing. It is well established that trace gas emissions vary widely on various spatial scales. For example, spatial variability of N_2O measured using chambers has been shown to range from 37 to 90% (*e.g.,* Hénault *et al.,* 1998; Laville *et al.,* 1999). Chambers, by their nature, are labour-intensive and time consuming. Integration through time and space is often a necessity and can be a large source of error (Rochette *et al.*, 1997).

1.2.4 The Nocturnal Boundary Layer budget technique

It is within the context of the nighttime regime that the NBL budget technique is now discussed. It is known that as the atmosphere becomes stable at night and exhibits a temperature inversion, GHG's emitted at the surface will become trapped and accumulate throughout the night. The NBL technique exploits this phenomenon by sampling trace gas concentrations from the surface through to the top of the NBL lid (inversion height or LLJ).

The NBL budget is calculated through a simplification of equation (1) by neglecting the turbulent component as

$$F_S = \int_0^z (\partial s/\partial t) dz + A \qquad (4)$$

In practice, a tethered helium-filled balloon makes ascents through the NBL while air is sampled for the appropriate GHG concentration. The difference in concentration for two different times is integrated over the height of the nocturnal boundary layer. Advection is assumed negligible as no practical method exists for routinely determining its effect. This assumption is valid for horizontally homogenous flat regions typical of agricultural production.

In contrast to eddy-covariance and flux-gradient techniques, the NBL technique is suitable (and, in fact, requires) very stable conditions. Accumulation under the NBL is larger than for the daytime case, thus making the calculation of fluxes easier (Denmead *et al.*, 1999). Usually, the height of the NBL has been defined as the point where the potential temperature becomes adiabatic. Although the NBL height is low compared to the daytime regime and makes measurement easier, ascents above 100 m can present difficulties in terms of instrumentation when strong winds (e.g. low level jet) are present. Furthermore, the height of the NBL is less well-defined than for daytime and can result in misinterpretation (Denmead *et al.*, 1996). For example, the potential temperature profile may become nearly adiabatic at several heights within a single ascent (Pattey *et al.*, 2002). The evolution of the NBL depends on the atmospheric character, and so, the only nights truly suitable lie in the very stable case (based on Mahrt's (1999) classification). Due to the special nature of this nighttime category, the upwind footprint is harder to

define and could further lead to misinterpretation (Denmead *et al.*, 1999). Finally, regardless of faults and qualities, the NBL technique is really a complementary method to daytime flux and provides nighttime data for the very stable case when other techniques fail. Measurements of the three agricultural trace gases with the NBL technique have been shown to be consistent with values found with the eddy-covariance technique (Pattey *et al.*, 2002; Griffith *et al.*, 2002) or with chambers (Meyers *et al.*, 2001) for the corresponding suitable conditions.

1.3 The Nocturnal Boundary Layer (NBL)

During the day, the convective boundary layer is driven by solar heating. As the atmosphere just above the ground is heated up by the solar rays, convective cells form and maintain movement within the layer. After sunset, the heat lost continuously through radiation is not replenished by solar heating and net cooling of the surface ensues. The ground cools faster than the bulk atmosphere and, in turn, cools air in contact with the surface through conductance. This cooling cascades upwards through radiation flux divergence and this sequence leads to a temperature inversion (the normal state of the atmosphere is lapse defined as temperature decreasing with height). Some few hours after sunset (2 to 3 hours according to Adedokun (1997)), a fully developed inversion can be observed. Such temperature inversions form the basis of nocturnal stability (§1.3.2) and define the main character of the NBL.

While the residual layer that remains above the NBL maintains the daytime characteristics, within the NBL, vertical movement, and therefore turbulence, is suppressed. Without turbulent movement, waves can be observed in the NBL. A z-less

stratification is established as layers of the atmosphere get decoupled from the ground (Mahrt, 1999). Because of this, we may obtain different layers with properties that are homogenized horizontally over a few kilometers (Stull, 1988). As a result, a low level jet (LLJ) can form (§1.4.1) as the non-geostrophic winds meet with the geostrophic component creating a supergeostrophic wind that shapes the wind profile with a wind speed maximum (Blackadar, 1957). Consequently, turbulence moves from the top of this boundary to the ground and we have what Mahrt (1999) termed an upside-down boundary layer.

Other features are unique to the NBL. Surface drainage flows with speeds as high as 1 to 2 ms^{-1} may occur when the topographic slope is more than 1 m per 100 to 1000 m (Hastie *et al.*, 1993). A sea breeze can be observed in regions in close proximity to large water bodies (Lapworth, 2000) and fog may form on calm and humid nights. Subsidence characterizing high pressure systems that usually results in clear skies is proposed to play a role in the evolution of the NBL – at least for the top third of it (Carlson and Stull, 1986). It is also believed that the time-mean transfer of momentum and heat is almost zero over the whole NBL depth (Ohya and Uchida, 2003).

Most importantly for this study, gas emitted from the surface tends to remain close to the ground - accumulating under the strong stability throughout the night. In this sense, the NBL is behaving as a large chamber and the principals of chamber measurements may be applied to this atmospheric layer. This is the basis of the NBL technique which takes advantage of this phenomenon by estimating gas fluxes between two successive measurements over the entire boundary depth (Denmead, 1996).

1.3.1 Radiative cooling

The rate of radiative cooling should be constant during a calm, clear night governed by the constant net radiation flux density (e.g. Van de Wiel *et al.*, 2003). As a result, air temperature at the surface should decrease at a steady rate, however, it is influenced by the intermittent turbulence which mixes heat downwards. In fact, Blackadar (1957) pointed out the fact that above a height of about one meter, the rate of nocturnal cooling is too large to be accounted for by radiative or conductive fluxes as turbulent transfer would be associated with upward propagation of the inversion surface (Nieuwstadt and Tennekes, 1980). Clear air radiative cooling was found to be on the order of 0.43 °C h^{-1}, and even though it is more significant at night, "accounts only for 0.3 % of the magnitude of the gross radiative heat flux from the atmosphere at the Earth surface" (Surridge, 1990, p.1285). Gopalakrishnan and Sharan (1998) stated that the proportion of cooling due to radiative and turbulent effects is dependent on the wind intensity. Air temperature in weak wind ($3ms^{-1}$ geostrophic wind) conditions is more influenced by radiative cooling. Mahrt (1999) set a surface wind threshold of 1.5 ms^{-1} where higher winds destroy the inversion.

Garratt and Brost (1981) created a three layer separation to visualize cooling due to turbulence and defined the central layer, occupying most of the boundary layer (70% of the total height), as the one in which turbulence dominates over radiative cooling. This would mean that the central part of the NBL, and so, the general shape of the potential temperature profile, is driven by turbulence. The profiles are classified depending on their shape; mixed, linear and exponential (Stull, 1988). These shapes depend on the 'mixing level' in the layer which is determined by turbulence. Based on that classification, the

linear profiles prove to have a greater vertical mixing compared with the exponential shape. The change in the potential temperature profile could then be explained by the increase of turbulence created in the nose of the jet situated in the middle of the static boundary h_S.

1.3.2 Stability and turbulence influencing vertical movement

Many features can contribute to intermittent turbulence or can inhibit the vertical dispersion. Generally, vertical turbulent transport decreases with increasing thermal stratification (Mahrt *et al.*, 1998) if no other mechanical features create mixing. Regions where a strong inversion exists will discourage vertical propagation outside of wind gusts. Other nighttime features such as intermittent turbulence, waves and low level jets (LLJ) involve vertical propagation. Under stable conditions, eddy diffusivity is difficult to determine and is often overestimated. It is now known to be closer to the molecular diffusivity than the previous values given by literature (Chimonas, 1999). Here, stability and turbulence and their role in vertical dispersion are discussed.

Atmospheric stability is a state of equilibrium for the air parcels that constitute the atmosphere. If an air parcel is stable, it must be forced before it will move vertically, but will tend to go back to its original position once the force is removed (Ahrens, 1994) attaining thermal equilibrium with its surroundings. It is a fundamental tenet that warmer air tends to rise since it is lighter, while colder, denser, air descends. The change in internal temperature for a parcel is controlled by the gas law:

$$PV = nRT \qquad (5)$$

As pressure (P; kPa) on the parcel is reduced as it ascends, its volume (V; m^3) is increased and its temperature (T; °K) decreases; this defines the parcel's lapse rate.

During an adiabatic process, the parcel does not exchange energy with its surroundings. A temperature inversion, therefore, characterizes stability in the limit that its lapse rate (called the environmental lapse rate) is not steeper than the dry adiabatic lapse rate (in the case of an unsaturated air parcel) or the moist adiabatic lapse rate (for a saturated parcel). The measure most commonly used for stability is the bulk Richardson number (Ri_B) which is determined within a layer Δz as

$$Ri_B = \frac{g}{\overline{T}} \frac{(\Delta \overline{T} / \Delta z)}{(\Delta u / \Delta z)^2} \qquad (6)$$

where $\overline{T}$ is the mean air temperature within the layer (°K), u is the horizontal wind speed (ms^{-1}) and g is the acceleration due to gravity (ms^{-2}). Essentially, the Richardson number represents a measure of the proportion of the static stability (temperature gradient) to the dynamic instability (wind gradient or shear). The Richardson number does not allow the quantification of the stability *per se*, but gives the probable state of the atmosphere with bounds that were determined by experimentation. Typically, a critical value (Ri_c) of 0.25 is used as the point beyond which flow is laminar in nature. This critical number is used to determine atmospheric layers that most probably contain turbulence, however, Chimonas (1999) pointed out that the cutoff value of 0.25 for laminar flow is often offset in many observations of the NBL. For example, some observations of strong turbulent bursts for heat and momentum have been made for values higher or close to the critical level: 0.1 to 0.3 (Bange and Roth, 1999). Other studies have used a threshold of 0.5 for Ri_B values to examine different features related to turbulence (e.g. André and Mahrt, 1982). Radiative fluxes and mesoscale flows can change the Richardson number to a higher value than Ri_c, while a barotropic pressure-gradient or the coriolis force will not result in a change (Derbyshire, 1999).

Turbulence defines a state where vertical movement predominates because of the dynamic and/or static instability. Convection mixes the lower atmosphere and therefore turbulence acts to homogenize gas concentrations. Since stability is the basis of gas accumulation, the presence of turbulence will influence the validity of gas concentrations measured with the NBL technique. Turbulence can be divided into a few cases that characterize a night which can be used to provide insight into the processes occurring within the NBL. Acedevo and Fitzjarrald (2003) established a classification of calm nights with a threshold of the average wind gust of a maximum of 1 ms^{-1} and spatial standard deviation of temperature higher than 1.5 °C. From this classification they experienced 20 calm nights over 62 nights. Pattey *et al.* (2002) used a classification of calm vs. intermittent turbulent periods to better determine nighttime respiration rates over agricultural fields.

The classification of Marht *et al.* (1998) is the most widely used. It divides the stable boundary layer into three categories: the weakly stable, the transition stability regime and the very stable case. The transition regime lies between the two extremes and expresses the period under which the stability regime is changed. In the weakly stable case, turbulence, although small, is always present because of generally strong winds or weak temperature inversions (e.g. a cloud covered sky radiating toward the ground).

The very stable case has an intermittent turbulent nature independent of location (Marht *et al.*, 1998). The strong stability prohibits vertical mixing such that winds, with less friction between the stratification, will intensify and, in turn, generate shear and therefore, vertical mixing in both gradient and counter-gradient direction (Ohya and Uchida, 2003). These breakdowns correspond also with wind gusts at the ground; they

are believed to create exchange between the surface and the top of the NBL (Acedevo and Fitzjarrald, 2003). The stratification is broken during these events and the height up to which it still connects with the ground is named H_c (Acedevo and Fitzjarrald, 2003). Outbursts have been observed with the strength of about five times the averaged values of a specific scalar (Bange and Roth, 1999) and to extend horizontally at least one kilometer (Poulos *et al.*, 2002; Coulter and Doran, 2002) and, less often, up to 25 kilometres (Coulter and Doran, 2002). It is known that intermittent turbulence influences the distribution of sensible heat, moisture and momentum (e.g. Poulos *et al.*, 2002) and often observations of turbulent events will be done by examining the time series (Sun, 2004; Acedevo and Fitzjarrald, 2003) of scalars or their fluxes (Bange and Roth, 1999; Coulter and Doran, 2002). It is also believed that trace gases would be transported by intermittent turbulence (Acedevo and Fitzjarrald, 2003; Nappo, 1991). A correlation between sensible heat flux due to mixing (and thus turbulent breakdown) and the exchange of nocturnal CO_2 has been found (Hollinger *et al.*, 1994).

In one of five turbulent events associated with Solitary-like waves, Cheung and Little (1990) observed a potential temperature variation having a maximum of 2.8°C and extending from heights of 10 to 50 m caused by a change of 5.4 ms^{-1} and 60° in wind and 2.8 ms^{-1} in the vertical movement over a period of 7 minutes while Chimonas (1999) found a difference of 5 to 10°C during a 10 min event. Both of these events seemed to be created by waves, but some breakdowns have no large-scale origin, and as such are not usually widely extending horizontally (Coulter and Doran, 2002). Topography could also influence intermittency as wind direction parallel to the large-scale slopes would increase turbulence levels at the downwind elevation (Coulter and Doran, 2002).

1.3.3 Modeling flowfields, NBL depth, footprint and advection

Modeling the very stable boundary layer is made difficult because of the intermittent character and small scale of the turbulence that is present (Carslaw and Beevers, 2002). Techniques which have proven useful such as large eddy simulation (LES) fail for very stable atmospheres (Saiki *et al.*, 2000; Galmarini *et al.*, 1998; Sorbjan and Uliasz, 1999) where small scale resolution is important (Piomelli, 1999). At best, an oversimplification involving Richardson models can reproduce the very stable conditions (Derbyshire, 1999), but not the complexity of gas diffusion.

The depth and strength of the NBL, given by the temperature inversion, have been shown theoretically and observationally to increase with the square root of time (Stull, 1983; Brost and Wyngaard, 1978). Ideally, the theory suggests a smooth increase in NBL height over time (Nieuwstadt and Driedonks, 1979; Singal,1989). Surridge and Swanepoel (1987) found, however, that such relationships do not hold at all sites. Attempts have been made to model the z-less turbulence character, but major differences between model output and observations remain (Ha and Mahrt, 2001).

While knowledge of the NBL height is critical for the technique, it is also important to understand the horizontal upwind extent from which the trace gas originates. As one might expect, a source area will get larger and farther upwind as stability and/or height increases (Schmid, 1994). Even though the upwind extent of the footprint, and therefore, the scale of transport of trace gases, has been estimated as on the order of 1 to 5 km (Denmead *et al.*, 1999), the true order of magnitude of the value remains unknown. Corsemeir *et al.*, 1997 contend that it may extend as much as hundreds of kilometers. Markovian simulations suggest that the magnitude of the footprint peak is four and six

times lower in stable than in neutral and unstable conditions respectively (Leclerc and Thurtell, 1990). A model created by Kormann and Meixner (2001) predicts that the maximum crosswind integrated flux footprint should be at a distance of 41.7 times the measurement height and that half the flux length scale should be 68.5 times the measurement height for typical meteorological parameters based on analytical solutions of the diffusion equation (Schuepp *et al.*, 1990). In general such simulations are hard to validate because of the difficulty surrounding the measurement of small fluxes (Finn *et al.*, 1996). This debate aside, the large footprint remains an interesting scale for the study of areas such as farms as it can incorporate all elements of production (cropped fields, manure piles, animal enclosures etc.). The NBL provides a homogenization of the whole region studied and therefore includes point source emissions or 'hot spots'. While the importance of this is apparent for highly variable gases (N_2O and CH_4), this effect can be also important for CO_2 as Leening *et al.* (2004) pointed out in the analysis of different locations and conditions within the two OASIS experiments.

Moreover, the turbulence theory that describes the ability of large eddies to transport scalars between two different heights without deposition between those levels could apply at night as waves redistribute scalars (Chimonas, 1999). Most footprint or source area models are based on a version of plume dispersion within turbulent conditions and therefore are not valid at night. Variability in the wind direction can also influence gas concentration. Elting (1990) stated that gas concentration under light wind, but with large directional fluctuations, was reduced by a factor of four or more compared to straight plume conditions. The variance in wind direction also has a large effect on the lateral diffusion pattern and plume spread (Ohba *et al.*, 1990). Wind direction

fluctuations are larger under unstable conditions, but not for the case of light wind conditions when there is low frequency motions (Ohba *et al.*, 1990). This meandering that reduces gas concentration by dilution is believed to result from large two-dimensional eddies. Concentration time scale fluctuations were observed to be an order of magnitude longer under stable conditions compared to near-neutral (Mylne, 1992). A good gas concentration homogenization in the horizontal is therefore essential for the use of the NBL technique.

1.4 Features of the NBL

Nighttime stability permits the appearance of certain phenomena that could not be seen otherwise. First, because the average motion of the atmosphere is less at night, features that are perhaps hidden during the day, can be exposed. Secondly, the stability that is created is intermittent in nature. The new features created by the NBL, can in turn, influence it. Furthermore, each will affect gas dispersion and are therefore very important within the context of the NBL technique.

1.4.1 Low level jet

The development of a low level jet (LLJ) within the stable boundary layer is very common (Banta *et al.*, 2002). There are three interesting aspects of the LLJ in terms of gas propagation: it is intimately linked to turbulence in the NBL; it is a source of gas advection; and it has been observed to lead to gas accumulation. Andreas *et al.* (2000) definition of a LLJ states that the maximum wind should be higher by 2 m/s than the speed at the top of the deformation of the jet and the LLJ should be elevated, otherwise

the properties become different. This corresponds to the classification developed by Banta *et al.* (2002) where, for example, a "low moderate winds" case exists where the turbulence level overall is relatively low. Banta *et al.* (2002) also suggest that changes in the shear below the jet, and therefore turbulence at that level, could be due to changes in the height rather than the speed of the jet. The LLJ can extend from 5 to 150 km horizontally, but is slightly dependent of the terrain (higher winds over a flat terrain will tend to create a stronger LLJ) (Beyrich *et al.*, 1997). LLJ's seem to attain their maximum speed around 0600 UTC (Anderson and Arritt, 2002).

It is known that the strong stability enables the wind aloft to become decoupled from the surface and reach supergeostrophic wind speed (Blackadar, 1957). Any decoupling creates intermittent turbulence because of the "stability regenerating turbulence" cycle (e.g. Van de Wiel *et al.*, 2002a) where strong stability leads to an increase in wind speed which in turns creates more shear and turbulence which is finally dissipated once the stability is increased after the shear diminishes the wind speed. Because of this, the LLJ does not dissipate, but rather fluctuates throughout the night with a net growth. Although this wind shear is sufficient to allow continuous generation of some turbulence, the presence of a wind speed maximum at the top of the inversion assures that this generation is controlled, as opposed to the maximum wind speed found above the inversion that results in chaotic breakdowns (Blackadar, 1957). Also, turbulence created by shear above the maximum wind will propagate upward while turbulence generated underneath will be more likely stopped by the static stability (Blackadar, 1957) since the gradient is the strongest underneath.

The LLJ is of course transporting gases and faster winds will tend to advect gases instead of creating a homogenised layer. However, this feature has also been shown to increase gas concentration near the ground. In one study, SO_2 was found to accumulate in regions where no source of emission was present (Beyrich *et al.*, 1997). Additionally, it is thought that this pollutant could have been mixed down by the strong shear that the wind maximum creates (Corsemeier *et al.*, 1997).

1.4.2 Gravity waves

Another event very specific to the NBL is the observation of waves. Believed to be always present, the waves are nevertheless observable at night because of the low level of turbulence which would otherwise mask their presence. The NBL acts as a waveguide (Rees *et al*, 1998). Waves are known to transport sensible heat flux (Cheung and Little, 1990), momentum, as well as gases (Chimonas, 2002) over a few kilometers (Chimonas, 1999). They can also be responsible for the escape of gas under the nighttime build-up (Fitzjarrald and Moore, 1990). Waves are believed to be caused by shear instability (Chimonas, 1999) and this would occur close to the point where the Richardson number falls below the critical value of 0.25 (Lee *et al.*, 1997). Kelvin-Helmotz instability creates intermittent turbulence by the rolling and breaking of waves (Ohya and Uchida, 2003). Internal gravity waves have been observed in the middle and the upper parts of the NBL (Ohya and Uchida, 2003) and internal solitary waves have been observed as low as 15 m to as high as 500 m (Cheung and Little, 1990). Their presence can be detected, for example, by a time-series analysis of specific scalars (either measured directly or calculated), vertical movement, and the Brünt Vaïsala frequency.

They can also be directly observed from a basic graph of SODAR frequency return termed the SODAR facsimile or sodargram (Cheung and Little, 1990).

1.5 SODAR

SODAR stands for "sonic detection and ranging". This instrument permits a view of the flowfield of the atmosphere by transforming the frequency returned from a sound signal into individual wind speed components. To determine the three wind components, three beams are sent at the same time. While small scale inhomogeneities move with the wind flows, their travel time is smaller than their own evolution. Using Doppler-effect theory enables the determination of the mean wind velocity from the scattered frequency (Kallistratova, 1997). As a result, a neutral atmosphere does not provide optimal conditions for the use of the SODAR (Beyrich *et al.*, 1997). Sunsets and sunrises are periods where the SODAR data does not behave adequately and the data should not be used. It is well suited for nighttime studies because of the lower nighttime boundary (Coulter, 1997). Pattey *et al.* (2002) suggest that its usage in conjunction with the NBL technique would be an asset in defining the top of the NBL. The instrument does not have direct access to the motion value for the three axes, instead, an interpretation of the different components from slightly different position in space is found. For that reason, the calculation of quantities such as covariance is not appropriate. The presence of other sources than atmospheric motions in the returned echo is another problem that might arise when using the SODAR data. This is especially true at night when wind values are small and their variations are even smaller (Coulter, 1997). Larger turbulence events will tend to dominate the received signal and can lead to overestimation (Coulter, 1997). The

distinction between scales of what is observed and the background can be uncertain and this could also lead to errors in interpreting the return signal (Chimonas, 1999).

The SODAR is considered a euleurian measurement instrument which collects data only for the part of the 'plume' that passes within its beam width (Coulter, 1997). The fact that the SODAR only takes instantaneous measurements is another potential source of error, fortunately, multiple measurements when averaged can correct this. The resolution associated with the SODAR is on the order of 0.3 ms^{-1} in horizontal wind speed, 0.05 ms^{-1} in the vertical and 3° in wind direction (Zhou, 1997), but these values also depend on the desired resolution, the maximum height chosen and, specifically, the height investigated (the data from the first gate closest to the ground is found to be less accurate).

An interpolation from the SODAR echo-return error data can be made to obtain the top of the NBL (Stull, 1988; Engelbart and Bange, 2002; Beyrich, 1994; Beyrich *et al.* 1993) and this height is usually denoted as h_S. Such a trace gives a general idea of the temporal evolution of the depth of the layer and how well the stratification is maintained throughout the night. Since this height is given by the zone of turbulence and that we know shear generation is increased by the LLJ (Smedman, 1988), it is normal that it stays consistent with the maximum wind of the LLJ (as well as the maximum wind during the development of this jet: h_u). This height best represents the turbulent NBL depth (h_R) as given by André and Mahrt (1982). As mentioned previously, the lowest height where the potential temperature becomes adiabatic can also be used to infer the top of the NBL (Stull, 1988), but the resulting values are much higher and are best interpreted as the

surface inversion height (h_s). Agreement between h_s and h_i seems dependent on the individual night and conditions studied (Beyrich *et al.*, 1997).

SODAR facsimile records (a graph of the backscattered frequency intensity of the vertically pointing component) can give a lot of visual insight on the presence and persistence of waves as these are displayed as clear undulations in the strata of strong returns (Bull, 1997). The vertical cross section is very useful in itself since a lot of information can be interpreted using time series analysis. Cross correlation functions between neighboring height levels and cross correlation functions between different heights in relation to a fixed height can bring added insight.

Mini-SODAR's have many advantages over SODAR's for agricultural nighttime measurement. Their small size makes them easily transportable and they do not impose an undue physical restriction to the farm operations. The high frequency provides a better velocity resolution - generally two to three times greater than with conventional SODAR's - and less extraneous noise because of the narrower beam widths that facilitate comparisons with *in-situ* instrumentation (Coulter, 1997). The piezoceramic tweeter arrays permit the first measurement to be taken closer to the ground (as low as 5 m) (Coulter, 1997). The fact that this system is limited to a maximum height of 200 m makes it perfect to the NBL study where the maximum depth of the layer rarely goes beyond that point (Coulter, 1997).

1.6 Thesis format

Since the NBL technique depends on stable atmospheric conditions, a study of this flux calculation method implies a good knowledge of the nighttime properties. An

investigation of the dynamic and static stability, along with nighttime features, using NBL soundings and SODAR is presented in Chapter 2. These techniques when combined, offer a greater ability to define the NBL height (Objective 1). Different ways to define the height are explored. While it has been assumed that intermittent turbulence is important for vertical gas diffusion, Chapter 3 reports unique observations that indicate the presence of non-zero vertical wind speed thus implying that a percentage of emission may be lost (Objective 2). Observations for two complete nights of measurement are contrasted. Chapter 4 focuses on the observational implications of a changing source area (Objective 3). The concentration footprint to this point has not been clearly defined and yet has large implications for the analyses of the flux calculated with the NBL technique. The thesis culminates in Chapter 5 which summarizes the findings, discusses limitations and explores scope for future research.

Chapter 2. Observations of Gas Accumulation under a Low-Level Jet

2.1 Introduction

The Nocturnal Boundary-Layer (NBL) technique, first introduced by Denmead *et al.*, (1996), assumes that gases emitted from the surface accumulate within the nocturnal boundary layer. This technique represents an attractive method to determine fluxes averaged over a large area. In contrast with most other flux measurement techniques, such as eddy-covariance, the NBL method is mostly suited to calm and clear nights characterized by strong potential temperature inversions. Although the top of the nighttime boundary layer is often thought to be better defined than its daytime counterpart (Denmead *et al.*, 1996), the reliability of this NBL technique is questionable when the top of the nocturnal boundary layer cannot be easily determined.

In the context of greenhouse gas measurements, much improvement on flux determination needs to be done. Respiration, for instance, is poorly accounted for in the net carbon balance and nighttime emissions of CH_4 and N_2O are assumed to correspond to daytime values despite the different surface-atmosphere exchange processes in nocturnal conditions. This is mainly because of the difficulty in making nighttime measurements. Eddy-covariance is an easy and continuous method of measurement and is now the most common technique used to measure CO_2 in the scientific community. Nevertheless, the technique relies on the assumption that the lower atmosphere is in a continuous turbulent state. When turbulence is intermittent or not present, errors will result that get magnified once integrated over time to daily and annual estimates (Baldocchi, 2003; Moncrieff *et al.*, 1996). Screening for non-turbulent periods is

becoming common practice and during such periods, often missing data are replaced with averages taken during windy conditions. However, this may lead to an underestimation of the true values (Pattey *et al.*, 2002). The same principle holds for the flux gradient technique extensively used for the measurement of N_2O and CH_4 fluxes which therefore also becomes questionable under stable conditions. The use of the NBL technique may facilitate gap filling in GHG time series for the nighttime data.

Better definitions of what constitutes capping conditions for gas accumulation associated with a low level of gas leakage have yet to be investigated for the use of the NBL technique. Accumulation under low level jets (LLJ) as observed by Beyrich *et al.*, 1997 and Corsemeir *et al.*, 2002 offer the possibility that this feature unique to the nighttime atmosphere may be a stronger blocking mechanism than the potential temperature inversion alone. This Chapter reports on field observations of gas accumulation beneath the underside of LLJ's which were observed to develop over agroecosystems. Discussion of these observations is made in the context of the influence of the determination of the NBL height on the reliability of fluxes calculated using the Nocturnal Boundary Layer budget technique.

2.2 Methods

2.2.1 Site description

The data presented here were collected during two field campaigns during the summers of 2002 and 2003 over agricultural land. The study site in 2002 was located south of Ottawa, Ontario, Canada (45°23' N, 75°43' W). The balloon launch site was a 24 ha corn (Zea Mays L.) field surrounded by agricultural land (Figure 2.1a).

Figure 2.1a. Aerial photograph of the balloon launch site near Ottawa, ON used during the summer 2002 field campaign.

The terrain was homogeneous with a slight slope of 1 m over 800 m from west to east. In 2003, the study area was situated in Côteau-du-Lac, Québec (45°19' N, 74°10' W). The balloon launch site was a 20 ha pea field (Figure 2.1b) that had grown to 0.25 m in height when harvested in July and was surrounded by corn and vegetable fields. The terrain was flat with a slope of about 3 m over 1.5 km. The launch site was situated about 2.3 km north-west of the St-Lawrence River which is 1.5 km wide at that location.

2.2.2 Instrumentation

During each night of observation, balloon ascents of 20-25 minutes duration were completed. A tethered meteorological tower (AIR, Model TS-5A-SP, Boulder, Co) was used to make vertical soundings of windspeed, direction, potential temperature, humidity and atmospheric pressure. A light-weight, fast response CO_2/H_2O infrared gas analyzer (CIRAS-SC, PP Systems, Hitchin, UK) was also suspended from the balloon and co-located with the sounding instrument package. The IRGA sampled atmospheric CO_2 instantaneous concentration on every second vertical profile. The meteorological data was logged to a notebook PC every two seconds in real time via a RF-transmitter/antenna while the IRGA data was measured and stored every ten seconds within the unit and downloaded to the PC after each flight.

A mini-SODAR system (Scintec Inc, model SFAS, Tubingen, Germany) was used on site for a two week period during each summer field campaign (June 24 to July 8, 2002 and July 22 to August 5, 2003) and continuously measured the three components of the wind vector between 10 m to 200 m every 2 minutes in 2002 and 5 minutes in 2003 in 5-m vertical increments.

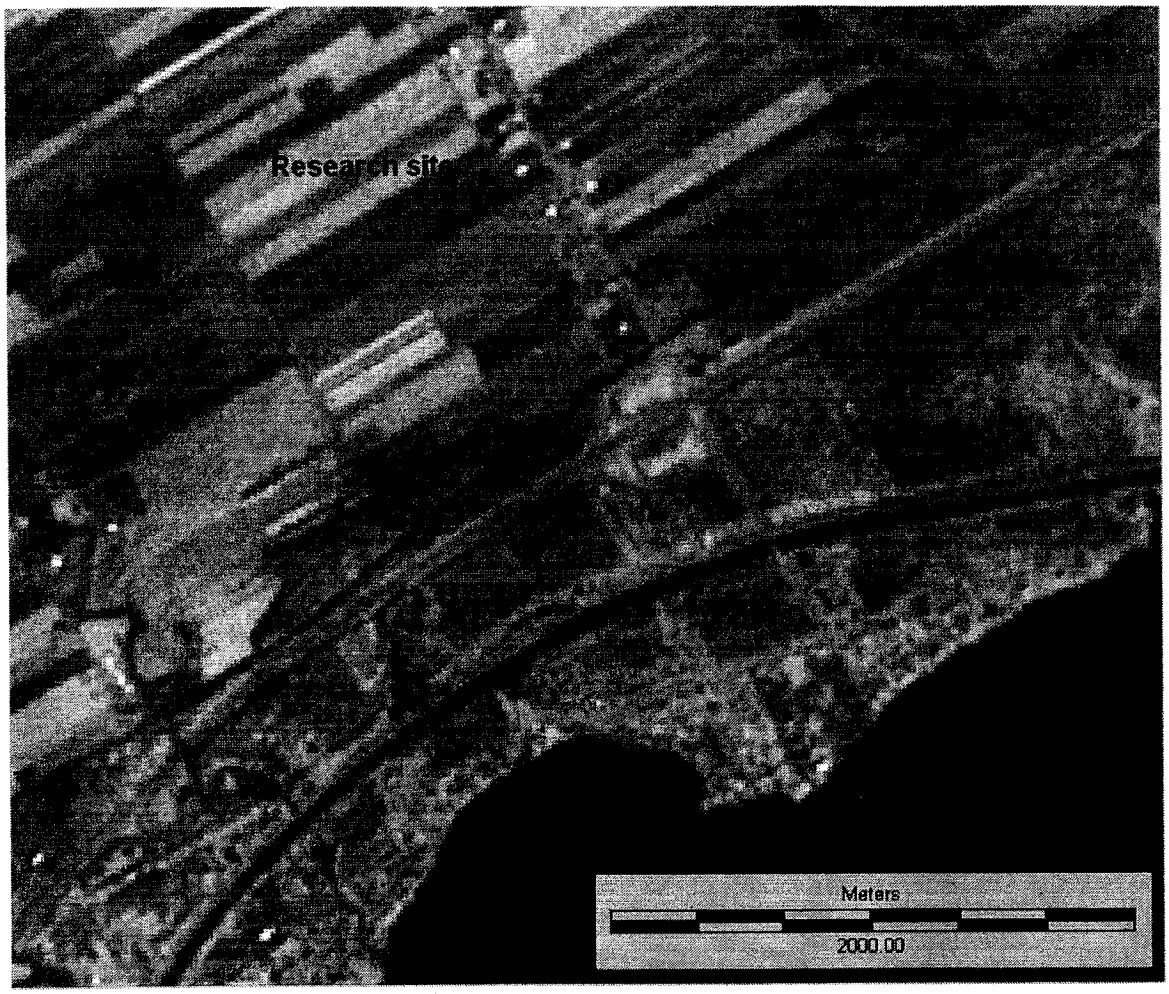

Figure 2.1b Satellite image of the balloon launch site near Côteau-du-Lac, QC used during the summer 2003 field campaign.

Basic meteorological variables were continuously recorded above the crop surface using standard instrumentation installed on a small tower and recorded by a data logger.

2.2.3 Decision making and meteorological conditions

Weather forecasts were used to screen synoptic conditions suitable for the NBL technique (i.e. conditions associated with a high pressure system, clear skies and winds below 1.4 ms^{-1}). For a three week period in 2002 and a 116-day period spanning May through September in 2003 conditions were monitored and information used to deploy the team and equipment to the field. These criteria resulted in seventeen partial nights and six complete nighttimes (from sunset to sunrise) of measurements. A summary of atmospheric conditions present during the measurement nights is provided in Appendix A.

2.3 Results and Discussion

2.3.1 NBL Height given by Static Stability (temperature inversion)

The NBL budget technique is predicated on the idea that the depth over which gas accumulates in a stable boundary layer (SBL) coincides with the NBL inversion height h_i (André and Mahrt, 1982). The field observations from this study suggest a far more complex picture: temperature inversions do not necessarily lead to gas confinement within the depth of the SBL as four of the six measurement nights refute this basic assumption. An example is given in Figure 2.2 where the profile of CO_2 concentration at 00:45 for the 28-29 June 2002 is observed to pass the temperature inversion height

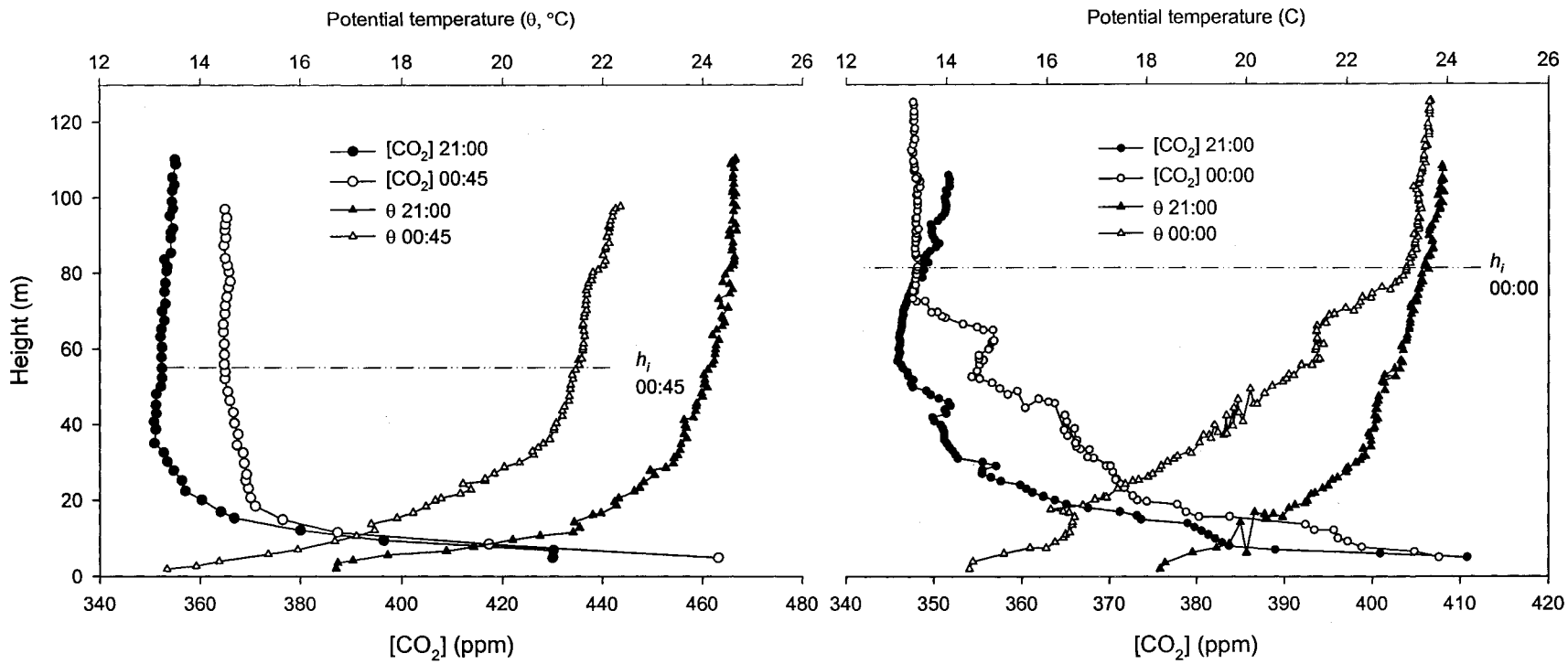

Figure 2.2 Potential temperature and CO2 concentration profiles for June 28-29, 2002 (left) and July 30-31, 2003 (right). The pair of profiles for the 28-29 June indicates that the CO_2 profile overshoots the top of the potential temperature inversion (dotted-dashed line) as the 00:45 EST profile never meets the 21:00 profile. In contrast, the profiles from the 30-31 July, 2003 demonstrate an accumulation, the top of which is defined by the temperature inversion.

around 70 m while never converging with the previous profile. In contrast, the example for the 30-31 July, 2003 profile of CO_2 concentration at 21:00 converges with the profile of the previous measurement. This indicated that on the 28-29 June, 2002 the accumulated gases were escaping the stable layer to blend with the residual layer concentration at a point above that at which the temperature profile became adiabatic. Since static stability diminishes with height, it gets easier for a gas parcel to escape the stability as it is moved up. At some point, dynamic instability takes over the static stability, the Richardson number becomes lower than the critical value (0.25) and vertical propagation occurs easily.

2.3.2 NBL Height defined by the presence of a LLJ

The depth of the NBL has been defined by many different characteristics of the NBL (Beyrich, 1997; André and Mahrt, 1982). For the NBL technique, the existence of a stable zone, which would lead to a barrier for gas dispersion, or any other mechanical mechanism that creates that barrier should be a good indicator of the height up to which measurements should be taken. Winds that are decoupled from the surface, and are supergeostrophic form a LLJ, the height of which is one means of defining the boundary layer. According to Andreas' (2000) definition, a LLJ is fully formed when the maximum wind is higher by 2 ms^{-1} than the speed at the base of the jet and that the latter is elevated. The wind maximum corresponds to h_u, but can also define the turbulent height h_R (André and Mahrt, 1982) at which turbulence is a maximum because of strong wind shear which is closely linked to the LLJ nose. A lack of echo return in mini-SODAR data given by this region of turbulence can be used to identify the NBL height.

During the night of 28-29 June, 2002, a strong LLJ was in place. The growth of the NBL as measured by mini-SODAR coincided well with the height of the nose of the LLJ as recorded by the tethersonde data (Figure 2.3). The rapid breakdown of the NBL and return of convective turbulence after sunrise is easily distinguishable beyond 0600 EST. Gases such as SO_2 have been shown to accumulate under the LLJ resulting in an increased concentration near the ground in the absence of a local source, advected source or downward mixing from the shear zone on the underside of the LLJ (Beyrich *et al.*, 1997; Corsemeir *et al.*, 2002).

2.3.2.1 Accumulation under a wind speed maximum

For any profile exhibiting a wind speed maximum, the majority of the accumulation of CO_2 can usually be observed from the surface through to the height corresponding to the base of the maxima. For example, on July 20-21, 2003, the highest level of accumulation was found under the base of the wind speed maxima in the profile and a decrease of CO_2 from this point up to the height of the maximum wind speed denotes leakage (Figure 2.4). A few other nights had a wind speed maximum too small in strength to be categorized as LLJ, but that still demonstrated blockage of CO_2. The wind speed does not have to be very strong to assist gas accumulation, but observations indicate that wind maxima that are steadier and closer to the ground (but detached from it) better act to retain gases underneath thereby preventing propagation above the wind speed maxima.

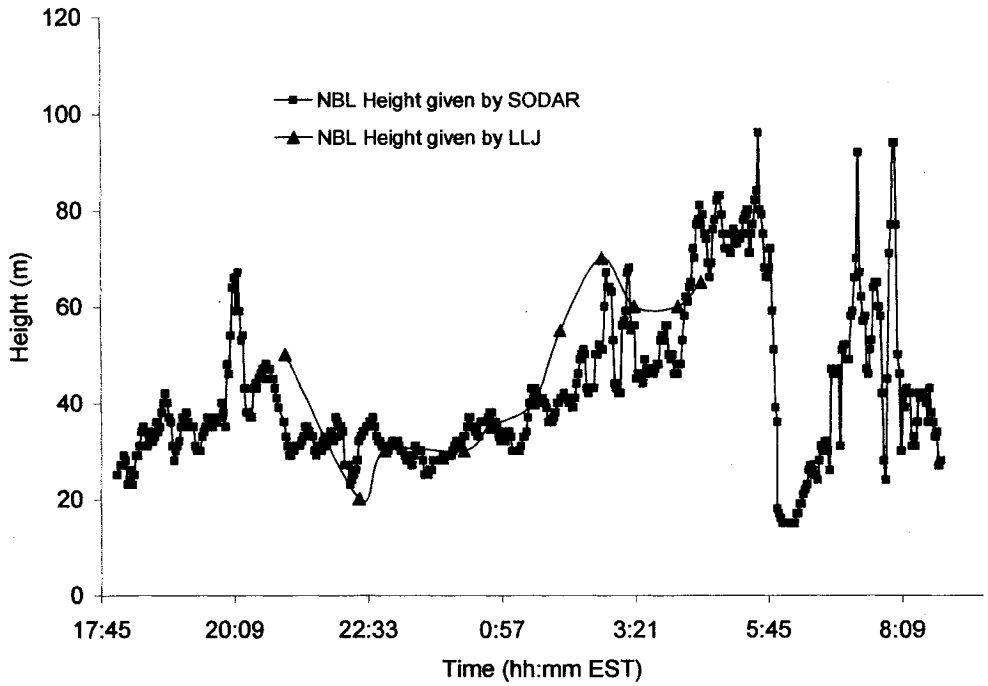

Figure 2.3 Height of the NBL for the 28-29 June, 2002 given by the mini-SODAR error return (pink) and the LLJ height as measured by the tethersonde wind profiles (blue). Sunrise is clearly distinguishable at 5:45 EST.

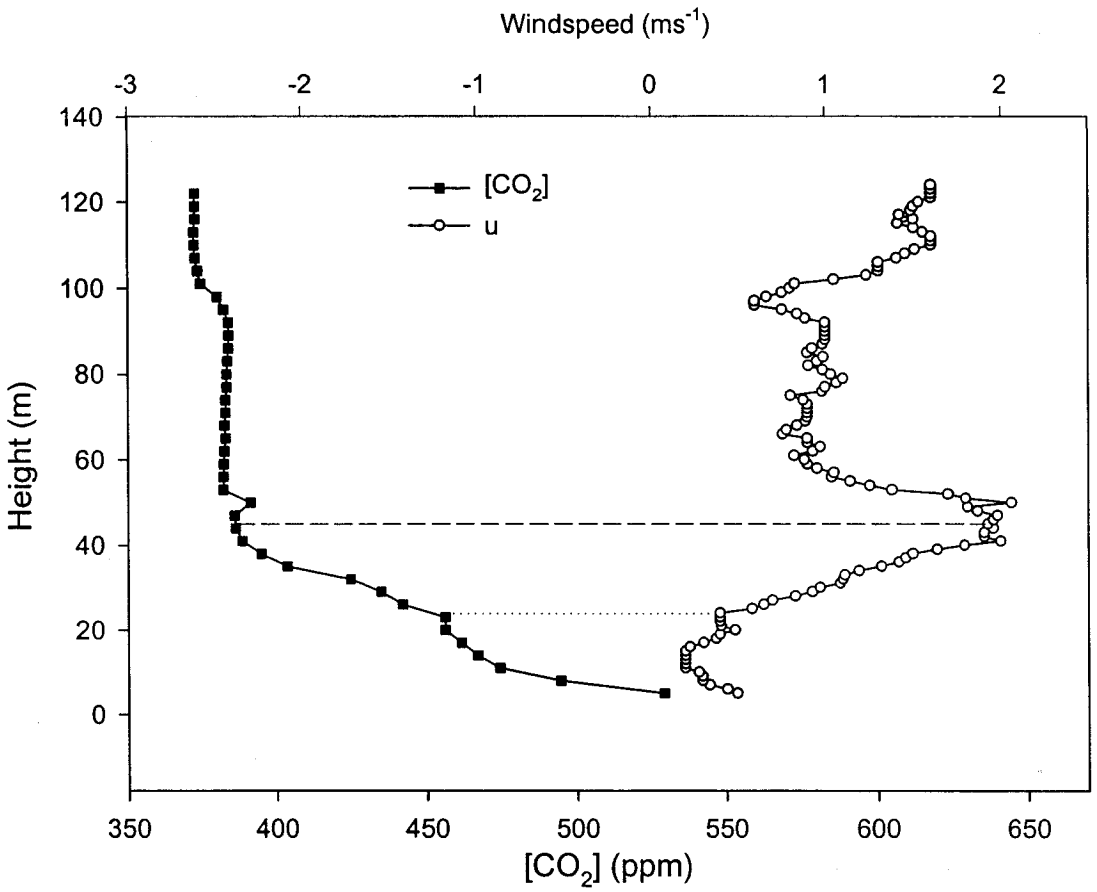

Figure 2.4 Observation of a wind maximum on 21 July, 2003 at 4:30 EST. The change in the CO_2 concentration gradient gives insight into the level of accumulation between each region. Gases accumulate easily under the level represented by the dotted line, at 20 m, which represents the base of the wind speed maxima. The concentration then decreases up to the height of the wind maximum represented by the dashed line.

2.3.2.2 NBL Height defined by the presence of a steady LLJ

From the current dataset, a good example of a steady and strong LLJ is the 28-29 June, 2002 where a LLJ was fully established during the period of the two final profiles and held the accumulating gas under the wind maximum (Figure 2.5). Profiles show an increase in the measured CO_2 concentration and vertical gas dispersion is inhibited. In the lowest part of the profile observed at 4:30 EST, the carbon dioxide accumulation is large because it has been conserved under a strong static stability. The constant concentration profile clearly indicates the height of gas accumulation to be around 40 m and corresponds to exactly the same level where the LLJ begins. This height also corresponds to the point at which an instability region is displayed by Richardson values passing the 0.25 threshold (Figure 2.6). There is dilution from 40 to 65 m within the underside of the LLJ corresponding to high turbulence levels generated by shear (Figure 2.5). The level of the LLJ wind maximum at 65 m corresponds to the point where concentration returns to that of the profiles measured earlier in the night (compare with 4:00 EST). The upper part of the LLJ maintained the same concentration throughout (65-90 m) suggesting that mixing has occurred. Since the concentration above 65 m is constant between the profiles, the assumption of no leakage through the LLJ can be considered valid.

It is important to point out that the LLJ for that night was 'controlled', with the region under 40 m always displaying similar wind profiles (Figure 2.7). It was found that the standard deviation of wind speed with time (σ_u) for measurement heights under the LLJ derived from mini-SODAR data was significantly lower than for the rest of the profiles, but also compared to the beginning of the night at the same heights. This LLJ is so constant that the demarcation with the underside is made clear. This region possesses

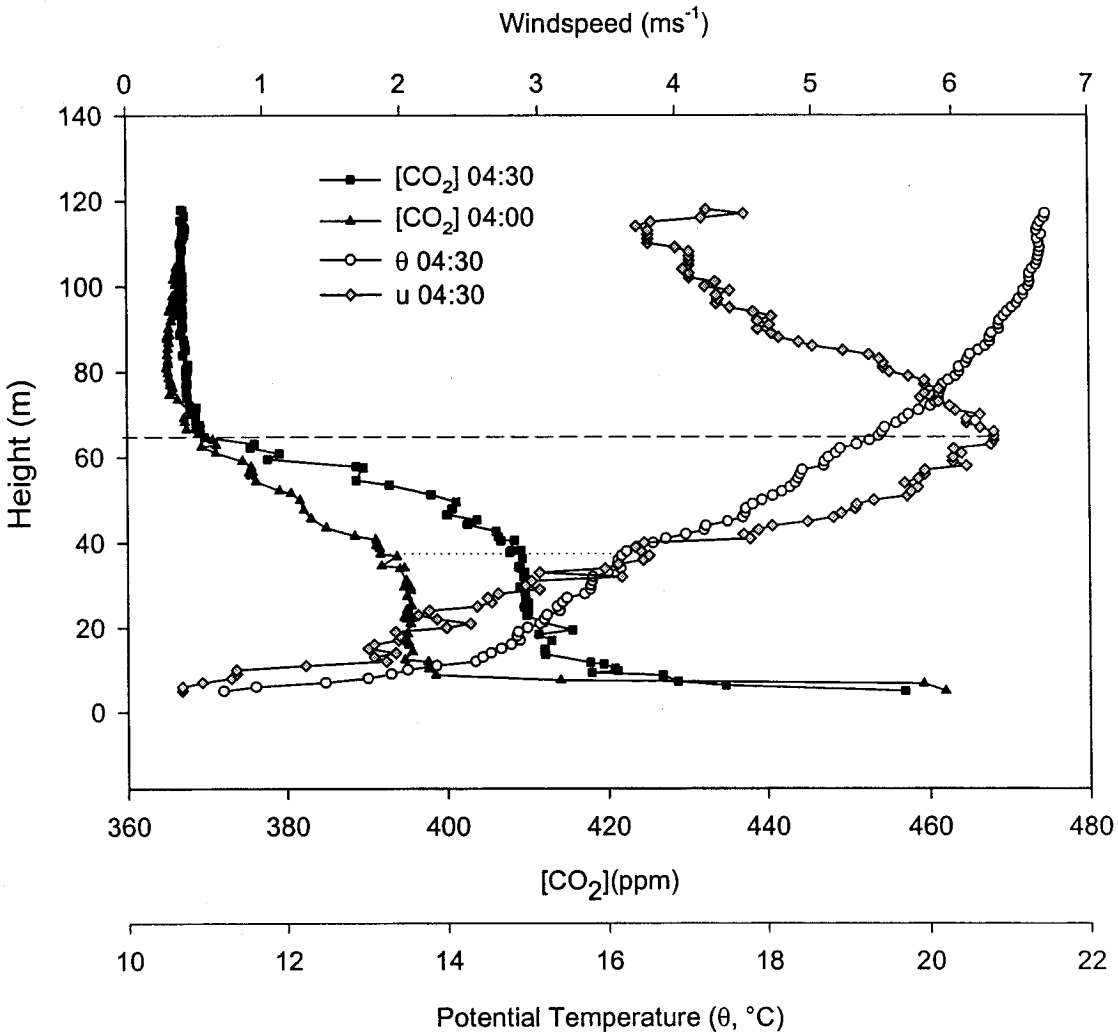

Figure 2.5 This pair of profiles from the 29 June, 2002 illustrates the idea of strong accumulation under the LLJ. The height of the base of the LLJ (dotted line) corresponds with the height at which concentration starts to decrease. The point at which concentration returns to that measured in the previous profile as the "background" concentration corresponds to the nose of the LLJ where the maximum wind is found (dashed line).

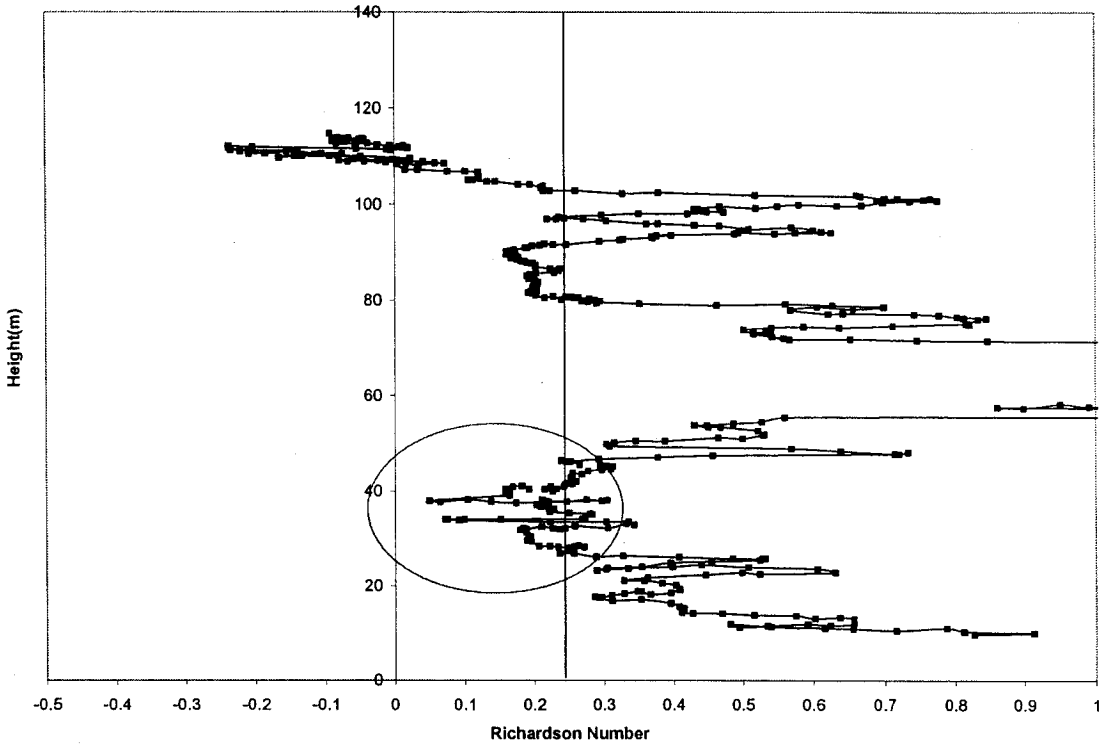

Figure 2.6 The Richardson number shows that the atmosphere within the NBL (under 80 m) is stable everywhere except at the base of the LLJ for the 29 June, 2002 during the last profile of 4:30 EST.

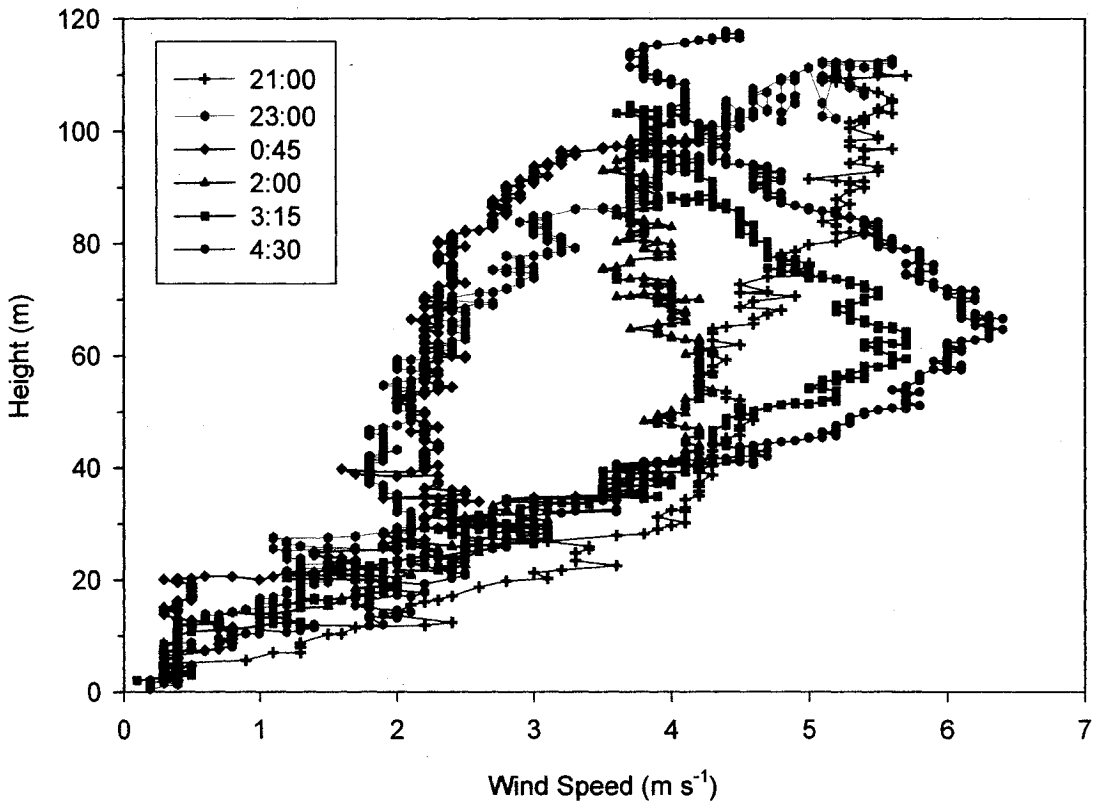

Figure 2.7 The different profiles of wind speed reveal the steady growth of the wind speed maxima for the night of 28-29 June, 2002. The consistency of the wind profile under 40 m height enables constant accumulation to occur. The wind maximum reaches its final height around 3:15.

greater variability and even if part of this variability is due to the lack of mini-SODAR data caused by turbulence, the standard deviation is still found to be less than that observed higher up or on other periods of the night (Table 2.1). The greatest standard deviation is found higher than the LLJ. The same applies for the standard deviation of wind direction with time at all levels (Table 2.1). The LLJ height was constant with time especially after 4:00 EST where instantaneous profiles almost always display the base of the LLJ at 40 m. The maximum observed wind speed was 6 ms^{-1} with a greater variation for the first hour of the LLJ. σ_u in this case was about 1.2 ms^{-1} and its height changed very little with time, mainly in the first hour after the jet creation. Using the mini-SODAR, it was often harder to define the top of the LLJ but this was likely caused by the poor quality of mini-SODAR data in the region of the LLJ because of the presence of turbulence.

If the wind maxima that is prohibiting vertical gas propagation is located in the lowest region where concentrations are already maintained by the strong temperature gradient, and is not coupled with the surface, it will not influence gas accumulation directly underneath by the creation of shear. Even though wind shear created from the LLJ was sufficient to allow continuous generation of turbulence, the fact that the wind speed maximum was located beneath the temperature inversion ensured that turbulence production was kept under control, as opposed to a maximum wind speed found above the inversion that results in chaotic breakdowns (Blackadar, 1957). In our study, the presence of a LLJ always corresponded with stronger gas accumulation well below the height defined by the top of the temperature inversion (h_i). A well-defined LLJ would decrease gas leakage and therefore uncertainties associated with the calculation of NBL

	28, 29 June, 2002		30, 31 July, 2003	
	Standard deviation of windspeed (ms^{-1})	Standard deviation of wind direction (°)	Standard deviation of windspeed (ms^{-1})	Standard deviation of wind direction (°)
under LLJ	0.32	9.5	0.35	30.2
underside of LLJ	0.45	8.4	0.71	12.1
upperside of LLJ	1.17	17.2	1.08	14.6
Higher than LLJ	1.79	61.5	1.54	24.0
Maximum windspeed height	0.37	6.1	0.88	21.5
No LLJ (averaged over all heights and time)	0.92	20.0	0.92	20.7

Table 2.1 Standard deviation of wind speed and direction in the different regions of profiles determined by the LLJ.

height would be minimized resulting in more accurate gas flux determination using the NBL budget technqiue.

2.3.2.3 NBL height defined by the presence of a less well-defined LLJ

Other nights were witness to wind maxima that could not be called a true LLJ according to Andreas' (2000) definition. Nevertheless, some of these wind maxima still had an effect on gas accumulation while others were too irregular to efficiently block vertical dispersion of gas.

On the 30-31 July, 2003, the winds were strong, but the maximum difference with geostrophic wind was not enough during the period from 3:30 EST to sunrise to be classified as a true LLJ. The high wind speed region almost reached the ground and so the lower limit of the wind maxima on this night (Figure 2.8) was not as evident as for the 28-29 June, 2002. This also means that the shear from the underside likely reached the ground and the strong accumulation that would have been present under the LLJ would become mixed within the region on the underside of the jet. Sub-critical Richardson numbers were observed for the first 25 m (Figure 2.9). This is the reason why no substantial gas accumulation is observed in the first 40 m from the ground as was the case for the well-defined LLJ (compare Figure 2.8 with Figure 2.5). The accumulation does not show the distinct "box" shape. Nevertheless, a distinct buildup of CO_2 was observed in the two last profiles under the wind maximum. The final concentration profile (4:15 EST) decreases rapidly from 30 to 40 m and then slowly decreases to a concentration of 373 ppm at the point it reaches 60 m - corresponding to the maximum wind speed (dashed line on Figure 2.8). A further decrease in CO_2 concentration can be

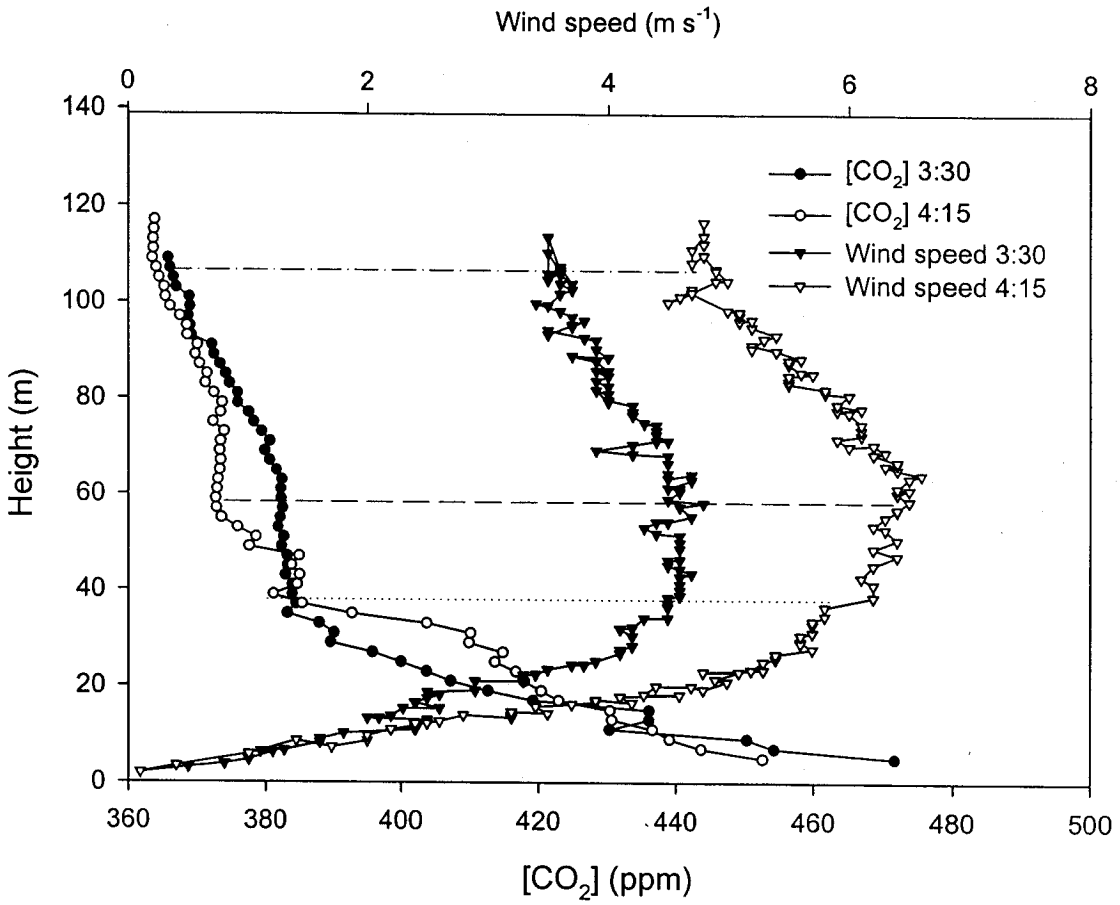

Figure 2.8 The LLJ on the 31 July, 2003 did not have the same capacity for trapping gas as did the LLJ observed on 29 July, 2002. Accumulation was still observed in the CO_2 concentration profiles - concentration decreases up to the region of the wind maximum (represented by the dotted and dashed lines). The decrease in CO_2 concentration between 50 and 110 m represents leakage.

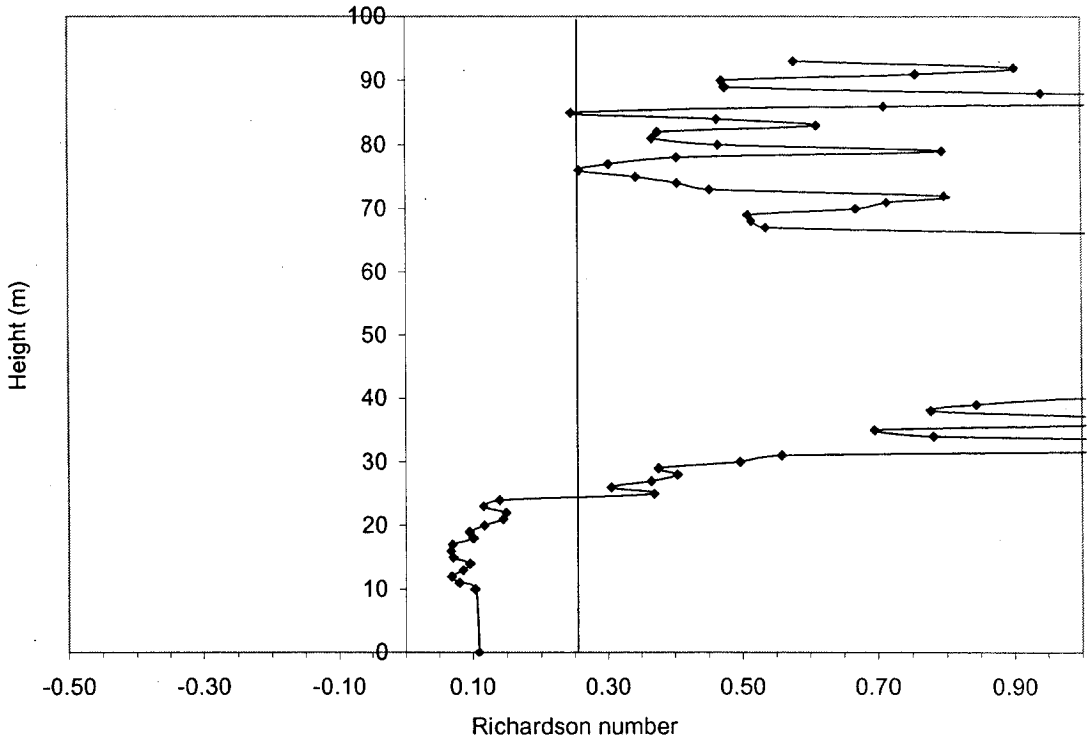

Figure 2.9 The Richardson number passes the stability threshold (0.25) for the first 25 m from the surface on the night of 30-31 July, 2003 at 04:15 EST. Since the LLJ is not decoupled from the ground, in this case, shear has more chance of reaching the ground.

observed from 80 to 110 m. This upper height represents the top of the LLJ at the time the profile was taken (dashed-dotted line on Figure 2.8).

Once more, the underside is the region where concentration decays to a constant value. The small standard deviation in wind speed close to the ground should represent the shallow region under the LLJ, although the variation is higher in the underside for this night compared to the 28-29 June, 2003. The statistics are similar between these two nights except for the standard deviation of wind direction which is much higher under the LLJ for the 2003 example (Table 2.1).

In 2003, the σ_u at the height of the wind maximum is larger than in the example from 2002 indicating the potential for more leakage. The maximum speed of 6.5 ms^{-1} observed from the tethersonde is given to be not more than 5.2 ms^{-1} from the mini-SODAR data. The height of the wind maxima is approximately 60 m from both tethersonde profiles and mini-SODAR systems and increases slowly from 45 to 60 m between the two last profiles. In the 2003 case, the height at which the LLJ terminates (upward end) is more consistent with time than what was observed in the 2002 case. The maximum wind speed is also more consistent in the 2003 case with a standard deviation of 0.5 ms^{-1} calculated from the mini-SODAR data (Figure 2.10).

For the 30-31 July, 2003, the two final CO_2 concentration profiles do demonstrate accumulation (Figure 2.8) The LLJ/wind maxima was so effective in blocking vertical gas propagation that accumulation started decreasing above the height of the wind maximum; not being replenished by gas leaking from below the LLJ. By integrating the difference between the CO_2 concentration profiles above the height of the maxima an estimate of the leakage can be obtained. The flux calculated between the two times over

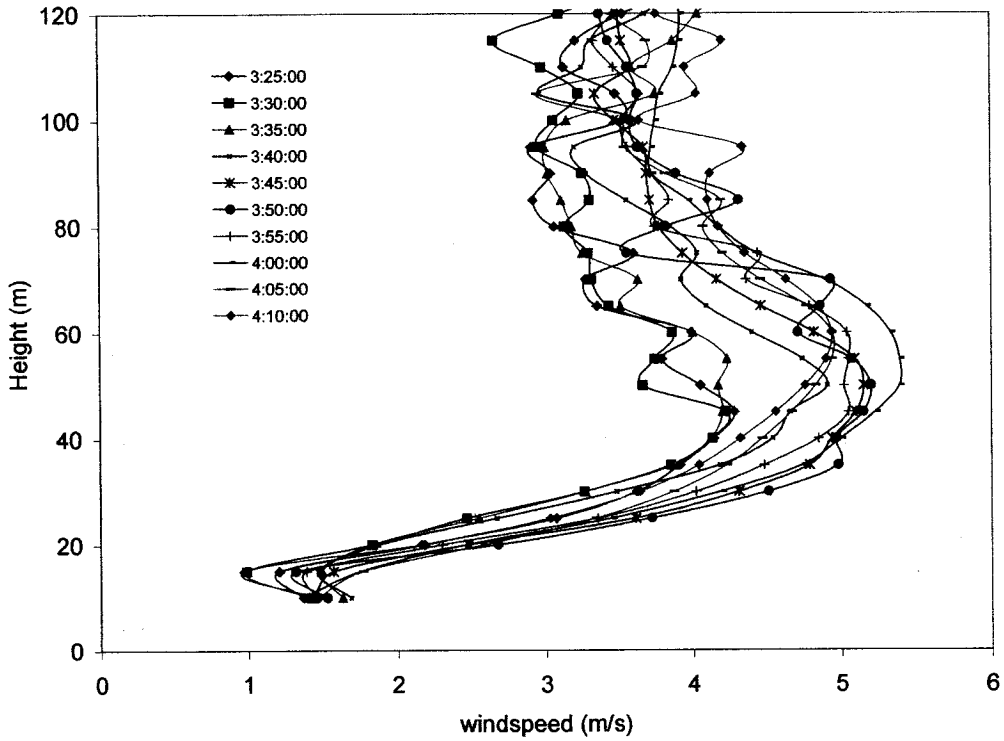

Figure 2.10 The mini-SODAR provides good knowledge at a 5-minute interval of the LLJ observed on the night of July 31, 2003. Note the consistency in wind speed, and the maximum wind speed height.

the height from 50 to 110 m is -0.18 $mgm^{-2}s^{-1}$ (Figure 2.8). It is suggested that this large flux provides evidence that this leakage is not only due to the normal leaking of the weak temperature gradient, but also to upward shear within the upper part of the LLJ. Blackadar (1957) states that turbulence created by shear above the maximum wind will propagate upward while turbulence generated underneath will be more likely stopped by the static stability since the gradient is the strongest underneath. It is evident from the 2003 case that the NBL flux should not be calculated using the whole depth of the NBL, but only the accumulation found underneath the LLJ or a strong wind maximum.

2.4. Summary and Conclusion

It has been demonstrated from different observations made during this experiment that the static stability does not act as a strong lid prohibiting vertical gas propagation on every night and is permeable to some degree in many circumstances.

The presence of a wind speed profile maximum or the development of a true LLJ affects the gas accumulation by impeding vertical dispersion. In the best case, when a LLJ is fully formed, gas propagation is blocked under it and the NBL technique is much more reliable especially if the wind maximum displays temporal consistency between two ascents and the wind maximum is fairly low in height staying decoupled from the surface.

It should be noted that turbulence driven by the shear created in the upper side of the LLJ accelerates the vertical dispersion of gas previously accumulated over the wind maximum. In this sense, when using the NBL budget technique, calculations should never be made using data from above the LLJ as the error will be magnified.

Preface to Chapter 3

In Chapter 2 observations of different types of accumulation was discussed. It was noted that CO_2 concentration profiles never met for some of the nights studied, while other nights showed a distinct cap for gas accumulation. Gases overshooting the temperature inversion are believed to get mixed rapidly in the residual layer leading to underestimation in the flux calculation of the NBL technique. Chapter 3 suggests that this phenomenon originates from an average vertical motion which maintains sign and strength over the entire NBL depth and throughout the night. Both chapters lead to a better knowledge of the suitability of nights for the use of the NBL technique.

Chapter 3. Continuous Vertical Motion Under the Nocturnal Boundary Layer and the Impact of Intermittent Turbulence

3.1 Introduction

The nocturnal boundary layer (NBL) possesses a stable nature because of the temperature inversion which builds through the loss of radiant energy from the surface. In the case of dynamic stability, gases propagate horizontally, trapped between stratified layers (Stull, 1988) and accumulate at the ground because of the suppression of strong turbulence and vertical mixing with gas at higher strata (Mahrt, 1985). In reality, perfect stability never occurs and the presence of stability intermittency observed within the NBL (Mahrt, 1989; Nappo, 1991) during very stable cases (classified according to Mahrt, 1998), will control the transport of different scalars such as heat, momentum and moisture (e.g. Poulos *et al.*, 2002). It has been suggested that this intermittency would also affect the vertical transport of gases and atmospheric pollutants (Acedevo and Fitzjarrald, 2003; Nappo, 1991). Much work has been done on intermittency (e.g. Nappo, 1991; Acedevo and Fitzjarrald, 2003; Mahrt, 1989; Van de Wiel *et al.*, 2002; Sun *et al.*, 2004) and on phenomena that either create, or are influenced by it.

Nighttime transport is of great interest to footprint modelers and scientists who study pollution transport (e.g. Pleune, 1990; Mazzeo and Venegas, 1991), but it is also important for the use of the NBL technique which assumes that gases emitted from the surface accumulate within the nocturnal boundary layer (Denmead, 1996). Gas diffusion is controlled by multiple atmospheric properties mainly based on two factors: static and dynamic stability.

In this Chapter, intermittency is investigated in the context of its potential impact on gas accumulation and the use of the NBL technique. An interesting feature observed during field measurements which will be termed the "background motion" is also reported as an average motion displacing air throughout the nighttime and the NBL height.

3.2 Methods

3.2.1 Site description

The experiment consisted of two field campaigns during the summers of 2002 and 2003 over agricultural land. The study site in 2002 was located south of Ottawa, Ontario, Canada (45°23' N, 75°43' W). The balloon launch site was a 24 ha corn (*Zea mays* L.) field surrounded by agricultural land (Figure 2.1a). The terrain was homogeneous with a slight slope of 1 m over 800 m from west to east. The immediate region contained farm buildings, agricultural land, treed patches and residential development.

In 2003, the study area was situated in Côteau-du-Lac, Québec (45°19' N, 74°10' W). The balloon launch site was a 20 ha pea field (Figure 2.1b) and was surrounded by corn and vegetable fields. The terrain was flat with a slope of about 3 m over 1.5 km. The launch site was situated about 2.3 km north-west of the St-Lawrence River which is 1.5 km wide at that location.

3.2.2 Instrumentation

The tethered meteorological tower and light-weight, fast response CO_2/H_2O infrared gas analyzer were described in detail in Chapter 2. A mini-SODAR system

(Scintec Inc, model SFAS, Tubingen, Germany) was installed in the respective field for each site at a distance of approximately 60 m from the main balloon launch site. The location was determined by the access to AC power supply and the desire to avoid the presence of solid structures (trees, buildings, balloon at its highest height) which would potentially contaminate the return signal. The mini-SODAR system includes 3 main units. The antenna/receiver consists of 64 transducers enclosed within a 0.25 m^2 case. This unit is connected to a processing unit which was protected from rain and small animals by a tent. The system is controlled by software installed on a laptop which also serves to collect the system output. Values from the mini-SODAR can be influenced by ground level noise for the lowest gates and therefore the antenna was surrounded by a 1.3 m high rigid metal shell with foam on the inside surface to absorb acoustic noise in the immediate vicinity of the sensor. This set-up permitted continuous measurement of the three components of the wind vector between 10 m to 200 m in 5-m vertical increments in real-time.

The mini-SODAR system was used on site for a two week period during each summer field campaign (June 24 to July 8, 2002 and July 22 to August 5, 2003). In 2003, it was necessary to remove and re-install the system to facilitate harvest of the primary crop and seeding of a forage crop. The system was also temporarily shut-down and removed from the power grid when a risk of lightning was present in the area.

3.2.3 Data processing

The most recent version of the Scintec software was not available in 2002 and each profile was an instantaneous measurement based on one set of acoustic beams. One

set includes five beams with one vertical beam and one in each of the four cardinal directions. This configuration resulted in a profile containing 39 data points (1 for each 5-m gate) being acquired every 1.92 minutes on average. In 2003, the software was upgraded substantially and the system was able to automatically average the results in an interval of 5 minutes. On average, this five-minute period was based on 2.5 complete sets of returns.

While the new version of the mini-SODAR software permitted real-time conversion of the data, the wind components using the 2002 data set had to be extracted from raw data files. An in-house Visual Basic program written by the author enabled the data to be imported into Excel worksheets to be reprocessed to obtain wind velocity and angle (direction).

The 2003 Scintec software reported very low levels of confidence for the first 20 meters at our field location. These values were subsequently not used in any calculations using the 2003 dataset.

3.2.4 Corrections to measurements

Because of the mini-SODAR's high resolution, vertical motion can be calculated with very low uncertainties given the proper installation; as low as a few millimeters per second under perfect conditions. The mini-SODAR was oriented North with a compass, and data were later corrected for the magnetic declination. During both years of measurement, care was taken to avoid tilting of the mini-SODAR acoustic system; a tri-axis level was used each time the mini-SODAR was installed in the field. If the mini-SODAR is properly leveled, a vertical sound beam is used to calculate the vertical wind

component (w). However, a tilt as small as 0.1° could lead in an error of 0.03 ms^{-1}. This error occurs because the tilt adds a systematic bias as explained below.

If the mini-SODAR is tilted toward the East at 90° and the real horizontal wind is flowing from West to East (inducing a positive horizontal wind component, u), the mini-SODAR software will identify w with the value of u such that the resulting vertical wind component (w') would be:

$$w' = 1.0 \cdot u$$

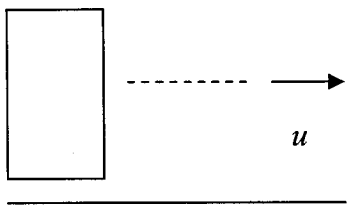

If the tilt is 45°, the result would be w' as half the value of u added to half the value of w as:

$$w' = \sqrt{(0.5w)^2 + (0.5u)^2}$$

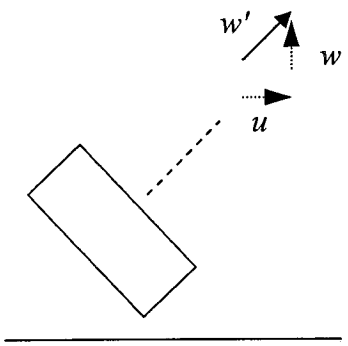

It is more likely that the error in the tilt would be around 1° giving:

$$w' = \sqrt{[(89°/90°)w]^2 + [(1°/90°)u]^2}$$

This implies almost a 1% addition of the value of u and a 1% decrease of the value of w to the calculation of w'. The magnitude of the error from w will be found to be small since values of w are small at night, but u can be quite large; for u = 5 ms^{-1}, the error added for a 1° tilt is 0.05 ms^{-1}. The above discussion refers to errors in the uw plane but could be expanded to include the cross wind component of the horizontal wind speed (v).

If there is a tilt, the error will always be proportional to the horizontal wind speed since the tilt would be constant throughout the night. If the error is of importance, we should never get w equals or close to zero for a large positive/negative value of u or v depending on the direction of the tilt. This is explored further in §3.3.1.

3.3 Results and Discussion

3.3.1 The absence of tilt effects

The values for w reported here are very small, and so a close examination of the data has been made for the presence of tilt effects. Since the field sites were so homogeneous and flat, the only possible source of tilt error was thought to be in a physical tilt of the antenna itself. As mentioned in §3.2.4, if tilt error is present, a correlation between the horizontal components and the vertical wind speed should be observed. For the night of June 28-29, 2002, on average, a net positive value for w of around 0.03 ms^{-1} was observed. The fact that it is consistent with height suggests that the proportional error with wind speed does not take place (as horizontal wind speed is unlikely to be constant with height and typically increases). Since, for most of this night, the wind is toward the S-E (u is positive and v negative), a tilt error could only come from a tilt toward East or South. In the case of large values of positive u and negative v,

w' should never be zero. 55 cases for which w' was measured to be zero were recorded from the 2490 measured values with u and v ranging as high as 5.53 and -5.91 ms^{-1}. The same observation was found for the 30-31 July, 2003 where an average negative w' of 0.08 ms^{-1} is observed. No significant correlations between u and w and v and w were found (Figure 3.1a,b) and therefore the hypothesis that a tilt effect is introducing bias to the observations is rejected.

3.3.2 Background vertical motion

It was noted in Chapter 2 that a temperature inversion may restrict the vertical dispersion of gases, but does not necessarily lead to complete gas confinement within the depth of the SBL. It was observed that on four of the six complete measurement nights, the accumulation of CO_2 overshoots the top of the inversion. This is illustrated in the different profiles obtained from July 18-19, 2002 (Figure 3.2). The accumulated gases were escaping the stable layer to blend with the residual layer concentration at a point above that at which the temperature profile became adiabatic.

Even though the potential temperature gradient plays an important role in restricting vertical motion, the main distribution of gas during the night does not depend on the overall inversion strength. Observational evidence made during this experiment suggests that the main upward migration of gases is controlled by an average vertical displacement (termed the background vertical motion), which maintains direction and strength throughout the night.

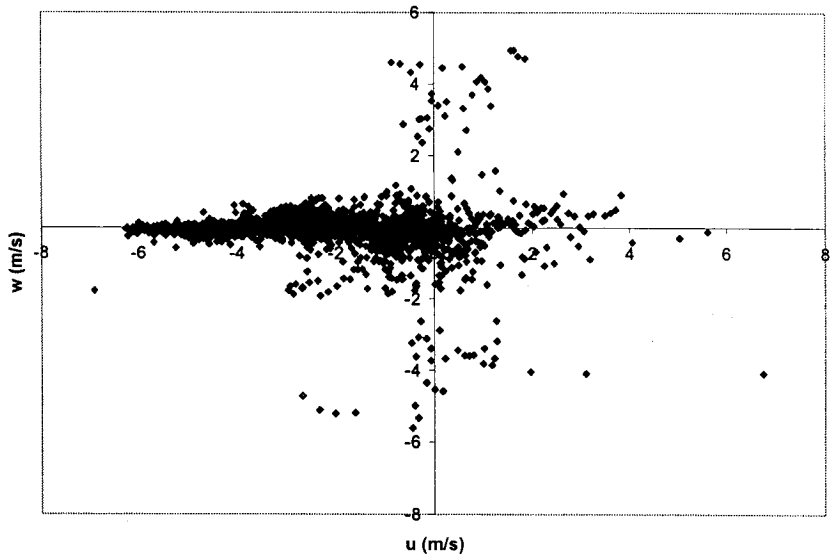

Figure 3.1a Scatter plot of the horizontal East-West wind speed component (u) and the vertical wind component (w) for all values found under the NBL. u and w are not significantly correlated as would be the case if a sensor tilt was present.

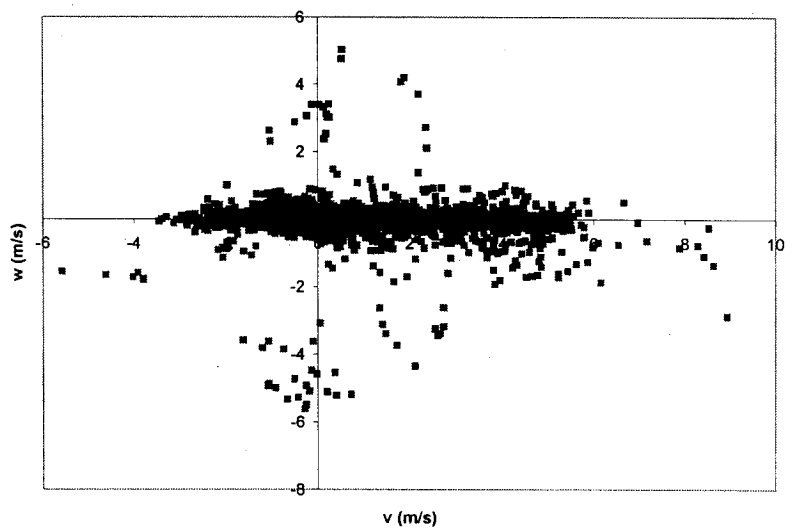

Figure 3.1b As in Figure 3.1a but for the North-South wind speed component (v) and w. No significant correlation was found.

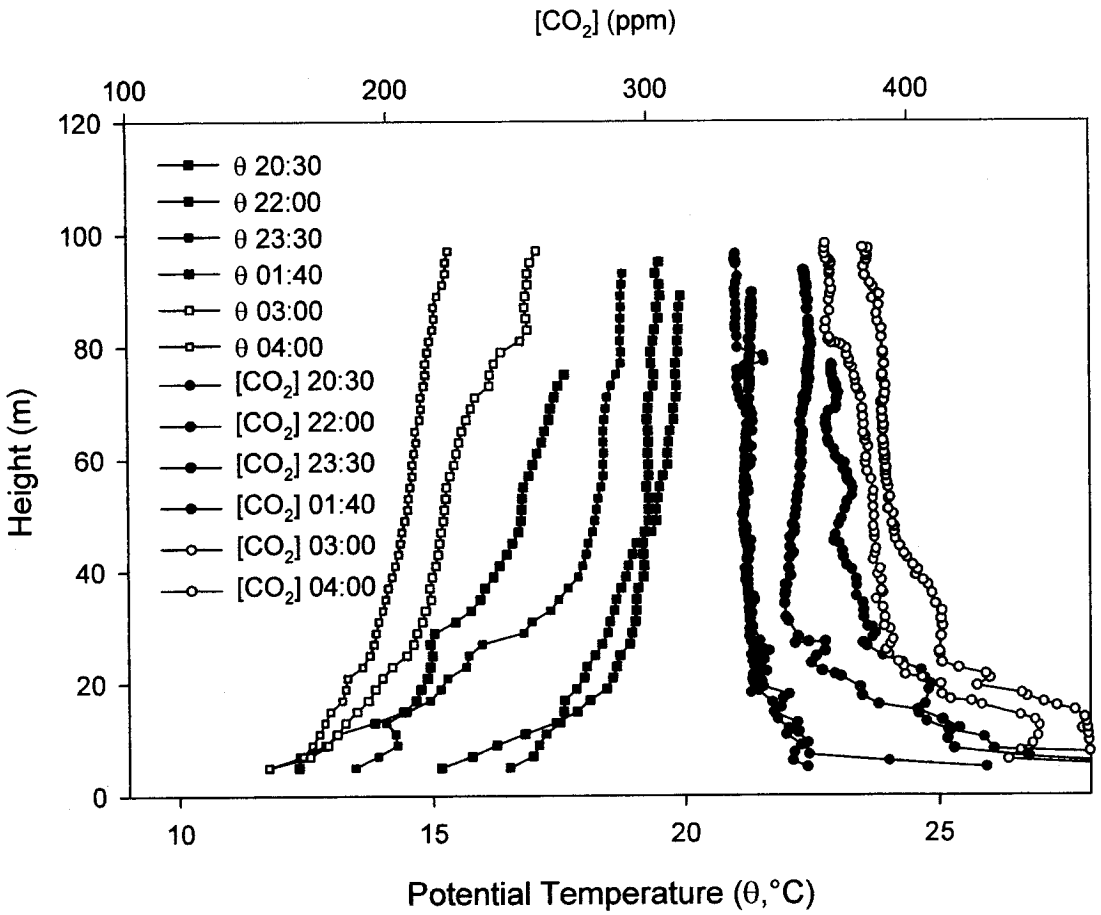

Figure 3.2 CO_2 concentration profiles taken on the 18-19 July, 2003 never meet, even if they pass the level of the potential temperature (θ) inversion (around 80 m) where accumulation should end.

3.3.2.1 SODAR observations: two cases

The presence of a background vertical motion was observed on two contrasting nights. The first night (28-29 June, 2002) represents ascending background motion while the second night (30-31 July, 2003) represents descending background motion. In Figures 3.3 and 3.4, the vertical wind speed component as derived from mini-SODAR profiles made during these nights is plotted for w values between -0.5 to 0.5 ms^{-1} where larger values are plotted darker. The reader will note the predominance of red indicating ascending motion on the first night (Figure 3.3) and the opposite predominance of blue indicating descending motion on the second night (Figure 3.4). Under ascending motion (i.e. Figure 3.3), throughout the night, carbon dioxide concentration profiles extend to a greater height before returning to equal concentration than they do under descending motion. Therefore, depending on this difference in vertical motion, gas will either accumulate and be mixed higher up in the residual layer or accumulate under the top of the inversion (h_i; André and Mahrt, 1982) thereby staying in the lowest part of the atmosphere where a strong potential temperature gradient still exists. The former situation (upward movement and mixing) implies leakage and therefore does not correspond to the ideal conditions for NBL measurements since the calculated fluxes can represent an underestimation of the true values.

Different thresholds were used to view this background vertical motion. For values limited between -1 and 1 ms^{-1}, (Figures 3.5a,b) it is obvious that the plot is dominated by the strong vertical motion in the residual layer. In fact, no values higher than 0.5ms^{-1} were present under the NBL height represented by the solid lines in Figures 3.3 and 3.4. Higher values of w were also present in the upper part of the wind

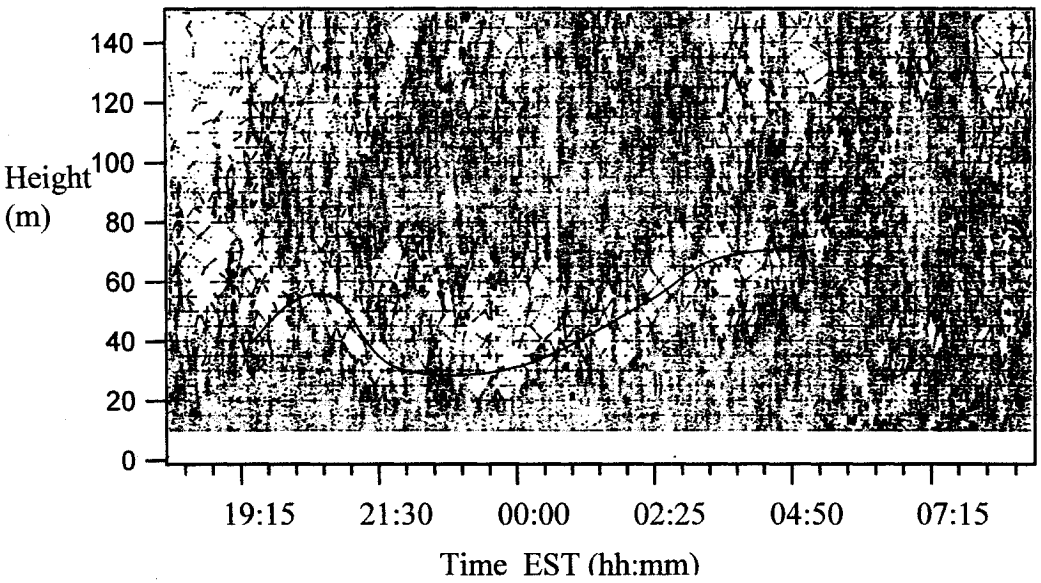

Figure 3.3 Vertical windspeed component (w) for the night of the 28-29 June, 2002. The solid curve represents a visual interpretation of the NBL height defined from the mini-SODAR error return data. w is plotted in the range of -0.5 to 0.5 ms^{-1}.

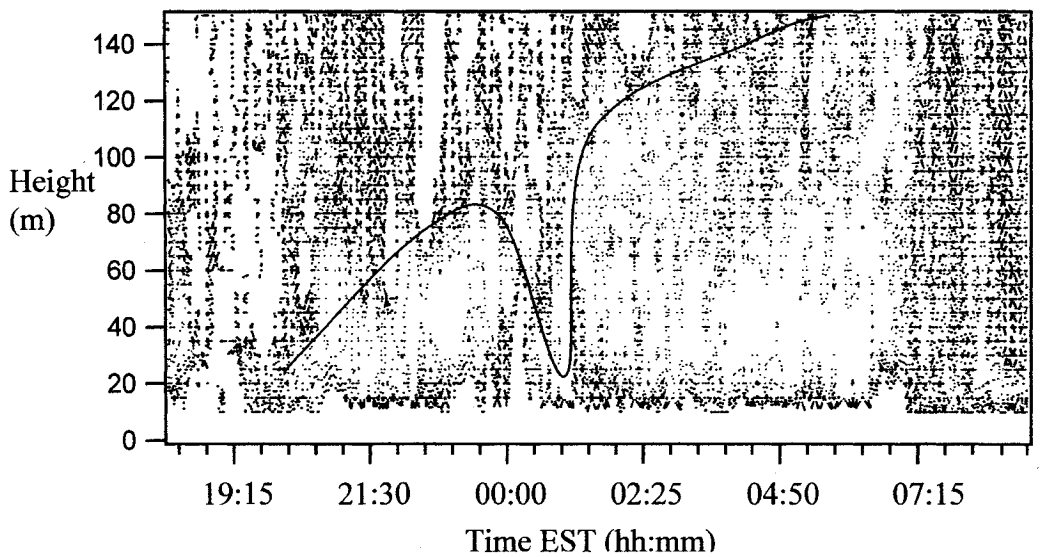

Figure 3.4 Vertical wind peed component (w) for the night of the 30-31 July, 2003. Negative values are blue and positive are red with the tone giving the strength of the variable; stronger colors being larger values. The solid curve represents a visual interpretation of the NBL height defined from the difference in strength of w between the residual layer and the NBL underneath. w is plotted in the range of -0.5 to 0.5 ms^{-1}.

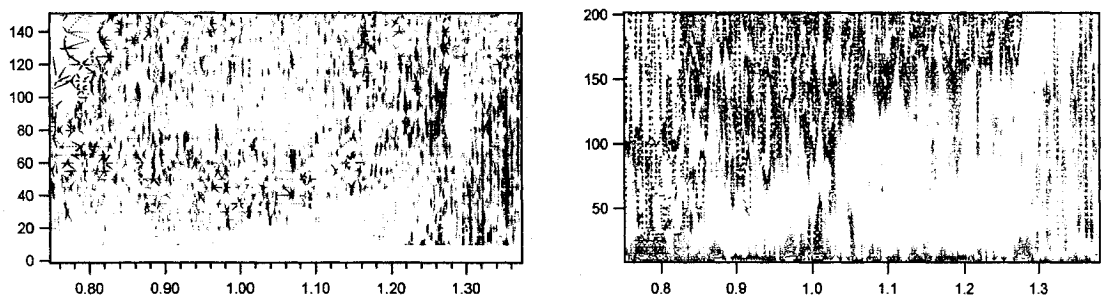

Figure 3.5a,b Plots of w similar to Figure 3.4 for the 28-29 June, 2002 (left) and 30-31 July, 2003 (right). A range of w of -1 to 1ms^{-1} was used. Note that most of the data is confined to the residual layer and that the white area indicates absolute values of w close to zero.

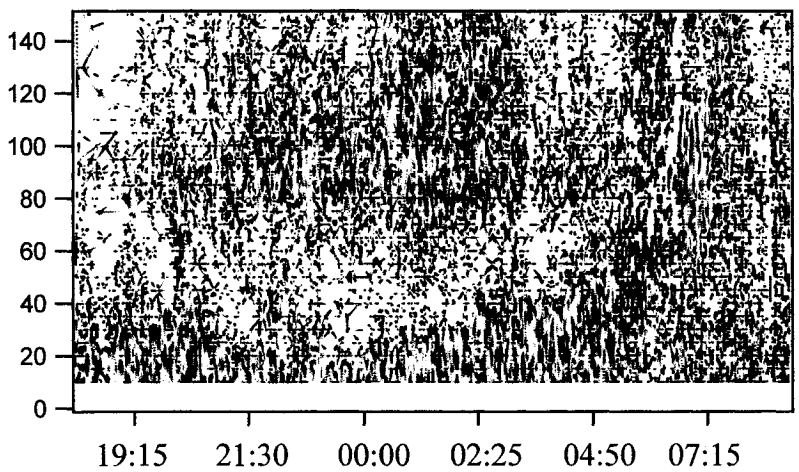

Figure 3.5c As for Figure 3.5a for the 28-29 June, 2002 using a range of (absolute) values for w of 0.2 ms^{-1}. Note the predominant ascending motion.

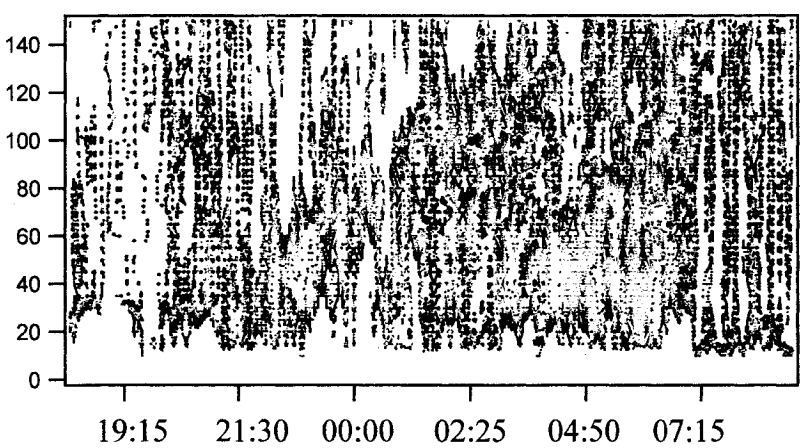

Figure 3.5d As for Figure 3.5b for the 30-31 July 2003 using a range of (absolute) values of w of 0.2 ms^{-1}. The majority of the observations are shaded blue (descending) even at these lower levels of w.

maximum/LLJ for the 28-29 June, 2003. Stronger values of w were also present in the upper part of the wind maximum (although lower than 28-29 June) for the 30-31 July between 3:30 EST and sunrise. For that night, larger w values are also observed for a period of NBL breakdown (described in Chapter 4) and for strong ascending motion representing the morning updrafts formed by solar radiation heating the ground. Since smaller thresholds permit observations on scales that would otherwise be masked by the larger (and less frequent) vertical motions, only values between ± 0.2 ms^{-1} are plotted in Figures 3.5c and d. Here, the predominant background motion (ascending for June 28-29 and descending for July 30-31) is more evident at various levels. The exception is during the 30-31 July, 2003 (Figure 3.5d) where slow ascending motion is observed around 2:00 EST.

3.3.2.2 Averaging

An average w of the entire night under the NBL height results in 0.03 ms^{-1} for the 28-29 June, 2002 and -0.08 ms^{-1} for the 30-31 July, 2003 with negative indicating downward direction. Averaging was based on 5-minute interval data for the 30-31 July, 2003. As mentioned previously this was a combination of 2.5 sets of mini-SODAR returns on average. The June 28-29 data was obtained from the raw output files and the interval was 1.92 minutes on average.

A visual appreciation of how the data varies with time can be seen in Figure 3.6. Averaging was done on smaller temporal scales to see if this average value was distributed evenly throughout the nights in question. At an averaging period of 20 minutes, the mean w already displays this background motion during some periods on a

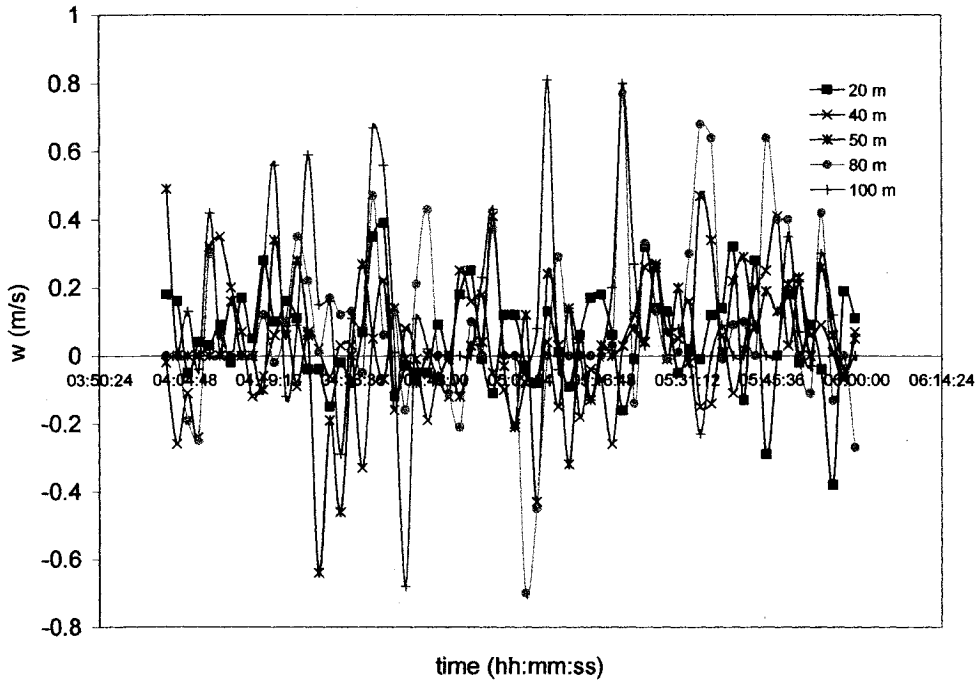

Figure 3.6 Raw data values of *w* for the 28-29 June, 2002 from 4:00 to 6:00 EST plotted for several heights indicate the variation of the data around zero. Most of the points can be found above zero where the background motion is for that night for each height series.

given night, typically for all heights under the NBL. Often, this average is surrounded by periods of higher values which will be later defined as turbulent events. To facilitate visualization, the *w* values were plotted as contours within height-time dataspace (Figure 3.7). This contour plot of *w* for a three hour period of 28-29 June, 2002, is a good example of the background ascending motion. There are periods of shorter duration that have larger *w* values. This background motion becomes more evident at higher averaging periods. It is further observed independently of time and height under the NBL which means that it is not an isolated observation, but rather a regional scale effect through time and vertical space.

3.3.2.3 Impact on gas accumulation

The background vertical motion is believed to be facilitating gas loss through the NBL when it is positive (indicating ascending motion). Gas accumulation higher than the temperature inversion corresponds to positive background vertical motion that would entrain gas in vertical dispersion. A small value on the order of 0.03 ms^{-1} would still correspond to the displacement of air of 3 cm per second. At this rate of movement, during the period between two ascents (typically 1 hour) the depth of displacement represents 108 m. This could lead to a huge impact in the distribution of gases and measurement using the NBL technique since the inversion rarely extends to much higher than 100 m in our examples. This background average motion does not imply the movement of gas at the same rate, but the result is certainly a loss of gas accumulation and underestimation of the flux calculated under the NBL. Further, the height of the NBL

cannot be exactly defined by the temperature inversion since it is suggested to be leaking and the amount lost in the

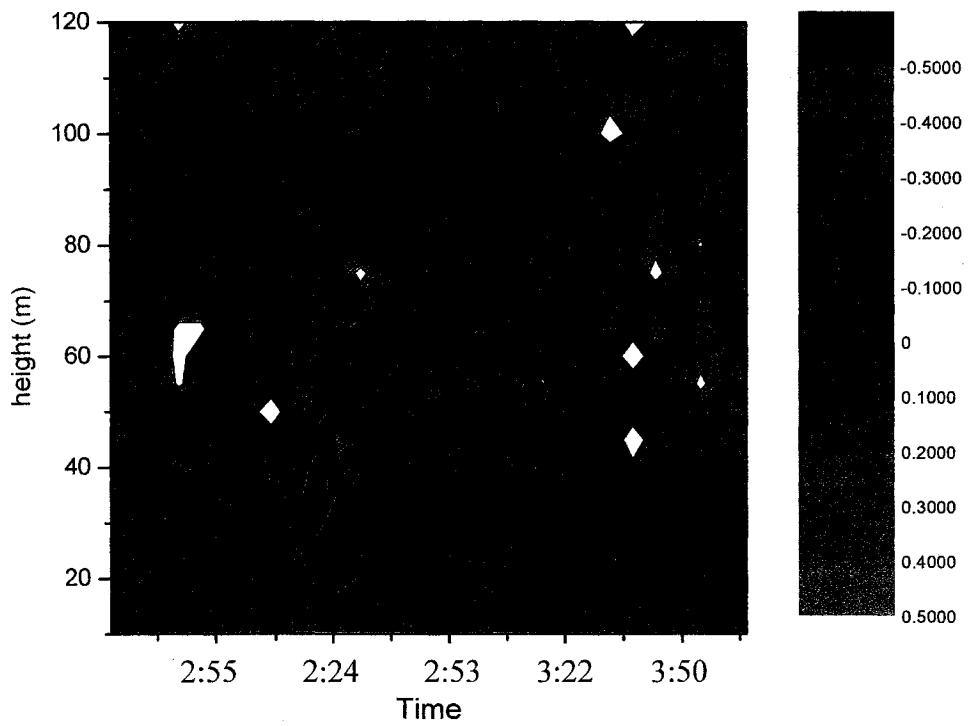

Figure 3.7 Contour plot of the vertical wind component (w) for a three-hour period of 28-29 June, 2002. The solid curve represents the height of the NBL. Note that higher values of turbulence (closed contours) surround this curve and are likely generated by shear around the LLJ.

residual layer cannot be calculated without errors because of the large turbulent intermittency in the residual layer.

3.3.3 Intermittency

3.3.3.1 Observations of turbulent events

It is strongly suggested in the NBL literature that turbulent intermittency occurring at night generates important displacements of gas and therefore corresponds to a large fraction of the overall gas exchange (e.g., Acedevo and Fitzjarrald, 2002; Nappo, 1991; Poulos *et al.*, 2002). Turbulent events have been observed in the past as changes in the temperature evolution or a sudden increase in wind speed. Two observations of increases in the temperature evolution have been observed during the night of June 28-29, 2002 from the ground up to almost 50 m (Figure 3.8). These strong turbulent events were confirmed to be non-local events (e.g. Poulos *et al.*, 2002) since the potential temperature data recorded from the meteorological tower (6 m above the ground and 40 m distant) displayed the same patterns (data not shown). Compared to other studies, these events can be considered of importance, but no link with higher values of vertical motion can be established. Intermittent motions found from the vertical motion data (where w is as large as 1.0 to 1.5 ms^{-1}) are located around h_R described as the turbulence height (André and Mahrt, 1986). This can also be seen in the w contour plot (Figure 3.7). This type of observation demonstrates the presence of what Mahrt *et al.* (1998) termed an upside-down NBL with the highest turbulent shear at the top. Outside of this, no evidence of events greater than 0.5 ms^{-1} under the NBL was recorded. Changes in wind speed and direction also have been examined, but, again no relation with w was indicated.

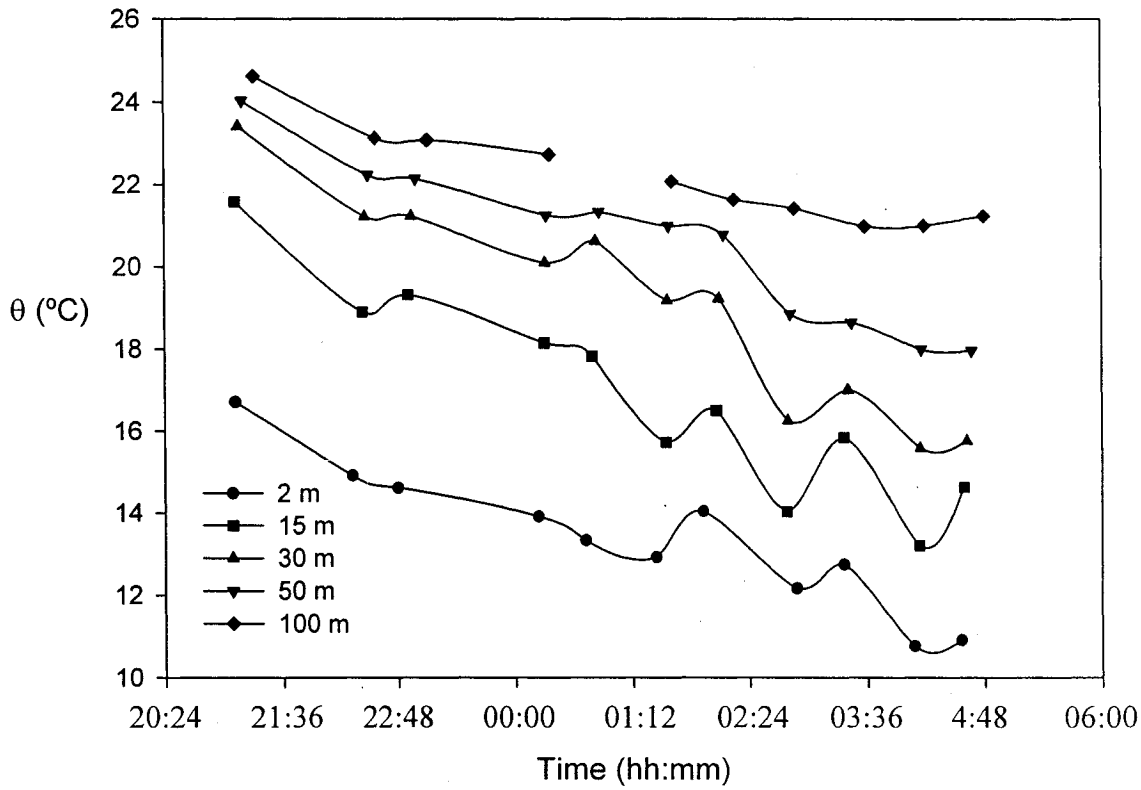

Figure 3.8 Potential temperature observations made by tethersonde ascents on 28-29, July, 2002. From the evolution of potential temperature for several heights two turbulent events are observed around 1:30 and 3:30 EST that disturb the normal decrease of temperature. These events were not located in the vicinity of higher values of w and are not believed to have had an impact on gas distribution.

3.3.3.2 Impact of intermittency

Turbulent events as observed in the nighttime temperature evolution did not seem to affect gas concentration directly, however, changes in the temperature profiles and especially the shape of those profiles, resulted in the modification of the gas concentration profiles. The breakdown of the NBL structure that was observed on three nights was primarily defined by a cooling throughout the layer that was larger than the radiative cooling of the ground (data not shown). These breakdowns are usually associated with vertical motion of absolute value greater than 1 ms^{-1} and are generally extending through the entire depth of the NBL. These are believed to be external events and should not be referred to as intermittent turbulence. The causes and implications of these external events were not explored in the current study and these were removed from the calculation of statistics and the definition of features explored in the next Section.

3.3.3.3 Statistics on intermittency

Basic statistics were calculated on instantaneous (5-minute average (2003) or 1.92 minute raw data (2002)) w data derived from mini-SODAR to determine the importance of intermittency for the two nights studied (28-29 June, 2002 and 30-31 July, 2003). Several thresholds were chosen: 0.05, 0.1, 0.2, 0.3, 0.4 and 0.5 based on the knowledge of the mean w of 0.03 and -0.08 ms^{-1} for 28-29 June, 2002 and 30-31 July, 2003 respectively and the maximum observed value of around 0.5 ms^{-1}.

Data within each of these thresholds exhibit the same percentage of positive/negative values (Table 3.1). Values for 2003 are 13% higher than for the 28-29 June, 2002 on average. That means that all ranges of w contribute to the sign of the mean.

28-29 June, 2002			30-31 July, 2003		
turbulence threshold (m/s)	percentage of data above this threshold	percentage of positive turbulence	turbulence threshold (m/s)	percentage of data above this threshold	percentage of negative turbulence
0.05	70%	62%	0.05	73%	70%
0.1	48%	62%	0.1	51%	74%
0.2	24%	62%	0.2	25%	79%
0.3	12%	63%	0.3	14%	78%
0.4	7%	59%	0.4	10%	77%
0.5	2%	67%	0.5	7%	75%

Table 3.1a,b Percentages of w values above different thresholds for the two nights as well as the positive/negative portion of these. The vertical direction by w is almost constant for different thresholds, but is different for each night. The night with the higher background motion, the 30-31 July, 2003, shows effectively a greater percentage of negative values.

In the same sense, the average absolute value of w (average strength of w in Table 3.2a,b), is higher by about 0.2 ms^{-1} for higher thresholds on the 28-29 June, 2002. The two nights display similar trends in cumulative frequency of w (Figure 3.9). This could be a means to designate stable nights. It turns out that around 50% of the data can be found above 0.1 ms^{-1} for both nights (Table 3.1a,b) and implies that this threshold is not a good indicator of intermittent turbulence, but mainly denotes data that are part of the background motion. As suspected, events higher in absolute value than 0.5 ms^{-1} are few; 2% and 7% of the data under the NBL in 2002 and 2003, respectively. The higher numbers for 2003 in general, reflect the higher average w.

It is hard to distinguish between turbulent events and normal changes in w (determine the intermittent turbulence) because of the even distribution in between each event defined by any selected threshold of w. The variation of w with time is large compared to the average (Figure 3.6) and so turbulent events have to be designated by the average variation of w around zero (average strength of w in Table 3.2a,b). This "amplitude" of the w data is around 0.20 ms^{-1}, it is then proposed that the turbulent threshold lies around 0.20 ms^{-1}. 25% of values of each night lie above this threshold. The average turbulence duration was three and nine minutes with a maximum of 12 and 50 minutes for 2002 and 2003, respectively. This also explains why the background motion can only be observed at longer averaging periods. The average duration of events (Table 3.2a,b) decreases as the w threshold increases to 0.2 ms^{-1} and stays generally constant after that. The 28-29 June, 2002 was more stable than the 30-31 July, 2003. On that night, there were more turbulent events but these were of shorter duration and had smaller vertical extent than were observed on the 30-31 July, 2003. Periods with the highest

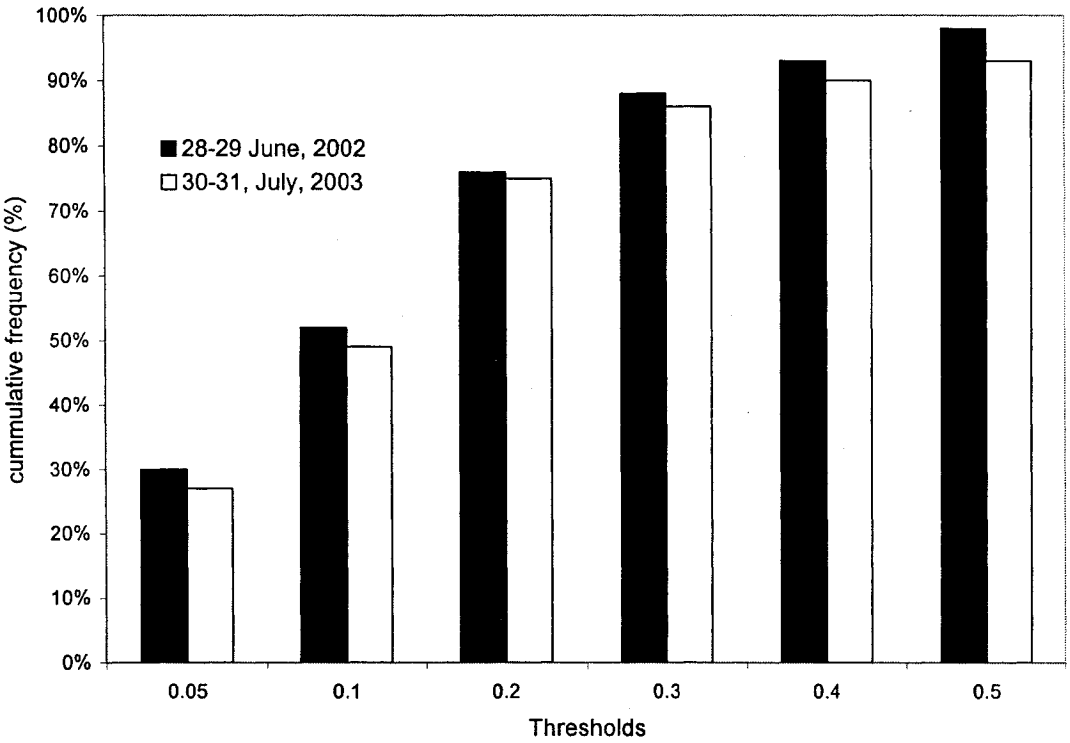

Figure 3.9 Cumulative frequency of vertical wind speed (w) for the two nights studied. A similar distribution is observed although a slightly higher percentage of values are found higher than the 0.5 ms^{-1} limit for the 30-31 July, 2003 which implies greater turbulence levels for that night.

28-29 June, 2002 under NBL (average: 32m) from 21h-06h					
turbulence threshold (m/s)	longest period (minutes)	average duration of event (min)	average # of events 5 m interval	average strength of w (m/s)	average w (m/s)
0.05	27	4.7	24.6	0.20	0.05
0.1	25	3.4	24.6	0.25	0.06
0.2	12	2.6	16.7	0.35	0.09
0.3	6	2.3	10.1	0.45	0.12
0.4	6	2.1	7.3	0.54	0.11
0.5	6	2.0	7.0	0.70	0.24
	maximum height extent (m)	average height extent (m)	average # of events per SODAR measurement period	height of highest number of events (m)	time of highest number of events (h:m)
0.05	70	11.2	2.1	15	5:37
0.1	45	8.2	2.1	15	3:15
0.2	30	6.4	1.7	25	5:35
0.3	15	5.8	1.4	25	4:31
0.4	10	5.5	1.2	25	4:24-5:03
0.5	10	5.5	1.1	40	22:35 & 5:31

Table 3.2a Important features of turbulence events are presented for different thresholds for the 28-29 July, 2002. Turbulence events occur higher than absolute value of 0.2 ms^{-1} where 25% of the values are situated.

30-31 July, 2003 under NBL (average: 87 m without first 20 m) from 21h-06h					
turbulence threshold (m/s)	longest period (minutes)	average duration of event (min)	average # of events per 5 m inteval	average strength of w (m/s)	average w (m/s)
0.05	130	19.4	12.7	0.23	-0.15
0.1	70	13.1	13.1	0.29	-0.15
0.2	50	9.1	9.3	0.45	-0.23
0.3	30	7.9	6.5	0.59	-0.30
0.4	30	6.9	5.5	0.71	-0.35
0.5	25	6.6	4.2	0.82	-0.38
	maximum height extent (m)	averaged height extent (m)	average # of events SODAR measurement period	height of highest number of events (m)	time of highest number of events (h:m)
0.05	130	28.4	3.06	30	1:55
0.1	110	20.8	2.9	65	3:45
0.2	65	15.7	1.9	85	3:55
0.3	30	12.9	1.4	85	3:50-5:35
0.4	25	10.9	1.2	145 & 155	<22h & >00h
0.5	10	9.2	1.0	155	00:35 & 3:50

Table 3.2b Same as Table 3.2a but for the 30-31 July, 2003.

number of turbulent events existed mainly around sunrise, but in general, more events were observed after midnight. A complete summary of these statistics is found in Tables 3.1 and 3.2.

3.4 Conclusion

It has been demonstrated from the different observations made during this experiment that the temperature inversion does not act as a strong lid prohibiting vertical gas propagation on every night and is permeable to some degree in many circumstances. Depending on the different structures of the atmosphere (background vertical motion), the gas accumulation will either remain under the top of the inversion h_i where the inversion is still strong, or it will accumulate from the ground up to a height where gas can escape the stability and meet the residual baseline concentration at a point higher than the top of the inversion (where one can assume strong mixing due to the residual instability).

Turbulent events are defined by a threshold of ± 0.2 ms^{-1}. All ranges of values participate in the creation of the background motion by their average, but also by their proportion of positive/negative values. It is suggested that the mean background motion is determined by absolute values between 0.05 to 0.15 ms^{-1} which should represent the average value found surrounding the error value. This background motion was observed to be constant in time and height under the NBL. Stability of the 28-29 June, 2002 has been found greater than for the 30-31 July, 2003 as its average event length is shorter, but a higher number of these with time is found on average for the night in 2002.

Turbulence, given by the w data, is relatively uniform during the night and is thought to contribute less to the transportation of gases than the background motion. The implication for the NBL technique is that gases will tend to escape the temperature inversion and cause an underestimation in the flux calculated.

Preface to Chapter 4

Chapter 3 reported gas leakage from an observed positive vertical displacement and its impact on the use of the NBL technique. In Chapter 4, horizontal advection is of concern as a change in wind direction is shown to lead to an overestimation of the calculated CO_2 flux through a change in the source area. The mechanism is suggested to be a density current leading to the temporary destruction of the stable layer.

Chapter 4. Breakdown of the NBL and its Impact on the NBL Technique

4.1. Introduction

The nocturnal boundary layer (NBL) builds at night under the temperature inversion created by the strong radiative cooling of the ground. The strong stability created by this temperature inversion inhibits vertical mixing and creates strata where horizontal homogeneity is maintained by the long length of time that gases spend in the same layer (Stull, 1988). In contrast, the convective boundary layer (CBL) during daytime is much deeper and contains very large eddies that carry energy and redistribute different scalar concentrations. The smaller fluxes at night make it harder to determine, model and verify the nighttime footprint (Finn *et al.*, 1996). Waves have been often observed in the NBL and are believed to transport gases (Chimonas, 2002). These features are of much interest in the study of pollutant dispersion but they can also have implications for nighttime measurement techniques. Lack of knowledge of the source area can lead to mistakes in the interpretation of a measurement, especially when using gas samples obtained at greater heights where winds are stronger and gases spend longer periods of horizontal movement in the same layer because of the slow vertical propagation. This horizontal transport enables observation of characteristics of distant source areas. It has been suggested that atypical potential temperature profiles that possess multiple heights at which the profile becomes adiabatic would designate a change in the source area; the same may hold for changes in CO_2 concentration observed with height (Pattey *et al.*, 2002). Circulation patterns like the land-sea breeze have also been reported to influence gas transport (Lapworth, 2000).

This chapter explores an observation of CO_2 concentration change due to a change in upwind source area. The causes and implications of this change are discussed in the context of the NBL budget technique.

4.2 Methods

This chapter focuses on the night of July 30-31, 2003. In 2003, the study area was situated in Côteau-du-Lac, Québec (45°19' N, 74°10' W). The balloon launch site was a 20 ha pea field that was surrounded by corn and vegetable fields. The terrain was flat with a slope of about 3 m over 1.5 km. The launch site was situated about 2.3 km north-west of the St-Lawrence River which is 1.5 km wide at that location. Profiles of potential temperature, relative humidity, wind speed and direction were made using a tethered meteorological tower as described in Chapter 2. A light-weight infra-red gas analyzer (CIRAS-SC) was suspended from the tethered balloon and measured profiles of CO_2 and water vapour. The Scintec mini-SODAR was deployed on site and made continuous measurements of the three components of the wind vector between 20 and 200 m as described in Chapter 3.

4.3. Results and Discussion

4.3.1 Observations of the disturbance within the NBL

On the night of the 30-31 of July, an event was observed around midnight which resulted in a change to the entire structure of the NBL. From the mini-SODAR derived vertical wind (w) time series, disturbances appear in the form of strong downward

motions (represented by darker tones in Figure 4.1) occurring around midnight (23h30 EST and 00h37 EST). Weaker disturbances (smaller w indicated by lighter tones on Figure 4.1) are observed at 21h45 and 01h40. The separation between the residual layer and the NBL underneath is clearly discernable because of the stronger vertical movement present. In this region, the temperature inversion is either not present or is not strong enough to maintain stability.

The observed NBL perturbation is of the same order as those in the residual layer with vertical displacement as large as -1.5 ms^{-1}. The perturbation seems to originate from the residual layer down to 40 m around midnight. Later perturbations seem to start around the 60-70 m level, with one extending to the ground and the other up to the residual layer. Around 1h40 EST and 2h20 EST ascending motion can be seen at the ground, but does not extend higher than 40 m.

A dramatic cooling of the air was recorded near ground level starting around 22h20 and lasting for about two hours. A strange evolution in the potential temperature was also observed at several other heights for that same night (Figure 4.2). Each episode seems to have occurred around the time the breakdown was observed. This cooling was recorded intermittently by tethersondes at the launch site, as well as in the continuous air temperature record of the meteorological tower some 60 m distant. This cooling is not as result of the normal nighttime evolution through radiative cooling as measured net radiation maintained a nearly constant negative flux throughout the majority of the night (Figure 4.3). Additionally, it cannot be explained by mixing from above as higher levels would be warmer and would have produced the opposite effect to the observed cooling.

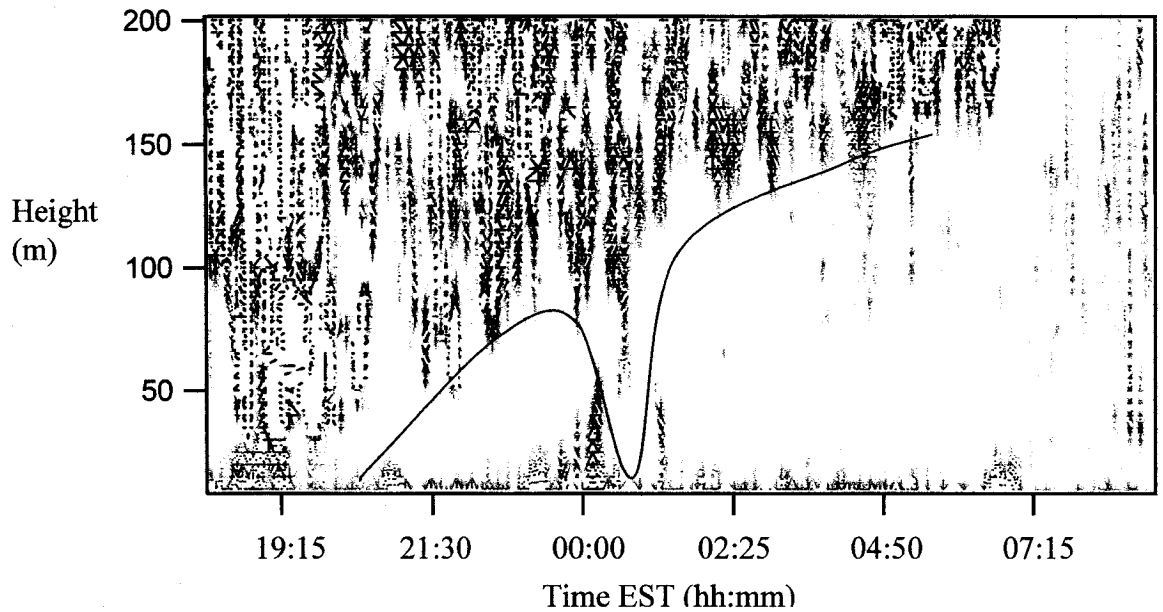

Figure 4.1 The vertical wind speed component (w) plotted as dots with positive values (ascending) as red and negative values (descending) as blue. The plot was generated using only data between -1.5 to 1.5 ms^{-1} to enhance finer details. Significant descending motion was observed around midnight. The solid line indicates the estimated NBL top as defined by the visual distinction between the strength of w in the residual layer and in the underlying NBL.

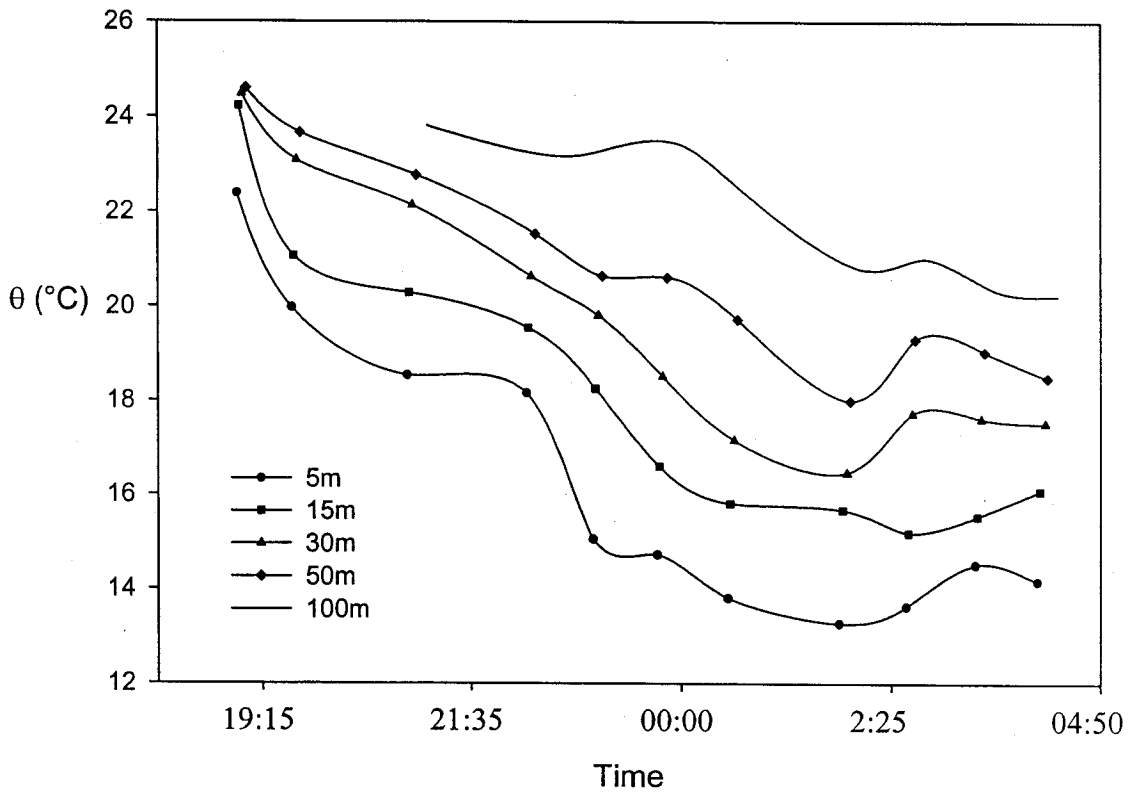

Figure 4.2 Potential temperature time series for several heights for the 30-31 July, 2003 as observed by tethersonde profiles. Note the change to the profile evolution during the time of the NBL breakdown.

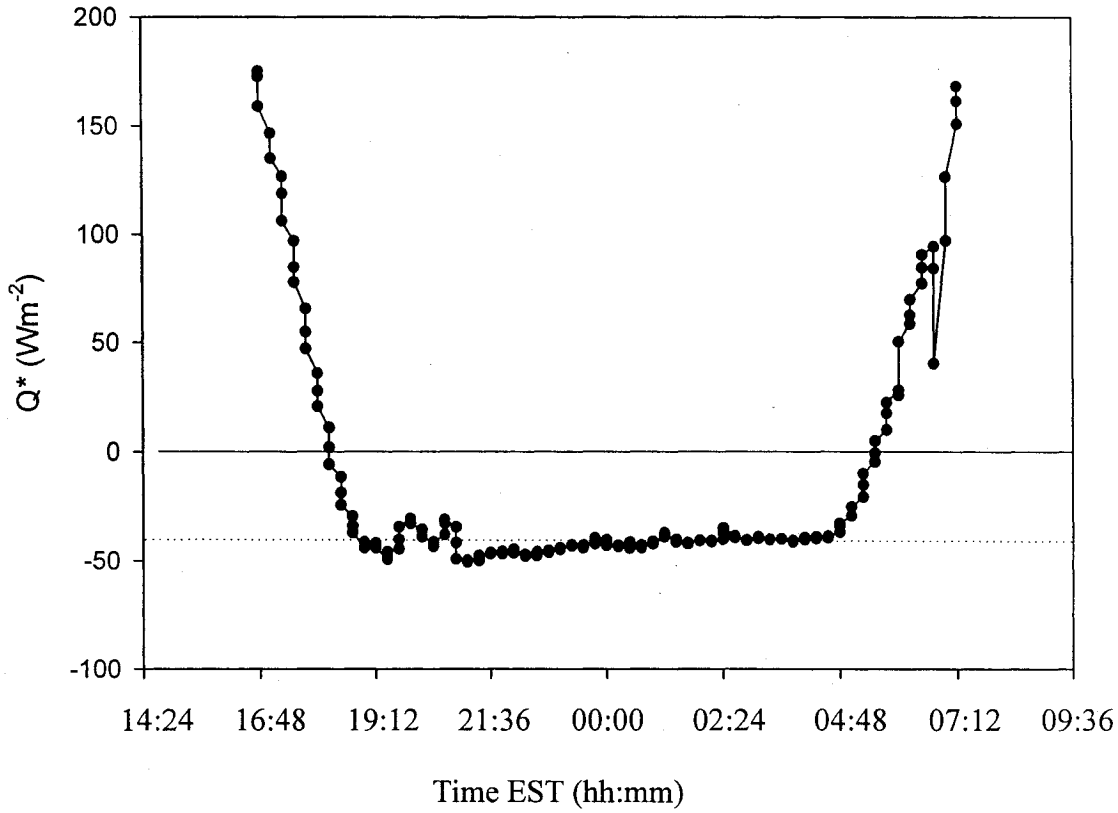

Figure 4.3 Net radiative flux density for the night of 30-31 July, 2003. No significant changes in the net longwave loss were observed throughout the period of the NBL breakdown.

The wind maximum that shapes the wind profile throughout the night followed the trend indicated by the mini-SODAR NBL height interpolation. It increased in height through to midnight, disappeared and then re-formed close to the ground subsequently to increase in height and strength (Figure 4.4). The disappearance of the wind maximum is believed to be closely tied to the breakdown of the NBL. One supposition is that the wind speed "bump" was diluted by the strong downward motion. Another possibility, since we know LLJ's are a controlling factor (Blackadaar, 1957), is that this disappearance could have lead the disturbance propagate through the whole NBL depth.

During stable nights, the bulk Richardson number (Ri_B) is typically larger than the critical limit of 0.25 throughout the NBL because of the potential temperature inversion. At times, shear increases and the atmosphere is more susceptible to shifts from the normal stability. During the observed event, Ri_B passes the critical number at a height of approximately 50-60 m (Figure 4.5). This coincides again with the height at which strong descending motion was observed to appear in the mini-SODAR data.

It was demonstrated in Chapter 2 that a wind maximum provides a solid cap to accumulation of gas. Since the LLJ was observed to vanish, one could imagine that this would result in a release of the accumulated gases that were previously trapped beneath the NBL lid. However, the observed increase in CO_2 concentration from the 00:00 EST profile to 02:00 EST profile (Figure 4.6) is larger than can be accounted for by the release and vertical dispersion of gases maintained up to 00:00 EST alone. Additionally, the increase is as large above the height of the previous wind maximum as it is at the ground. The resulting flux calculated over the period of the disturbance compared with other pairs during this night is too large to have resulted from the same source of emission.

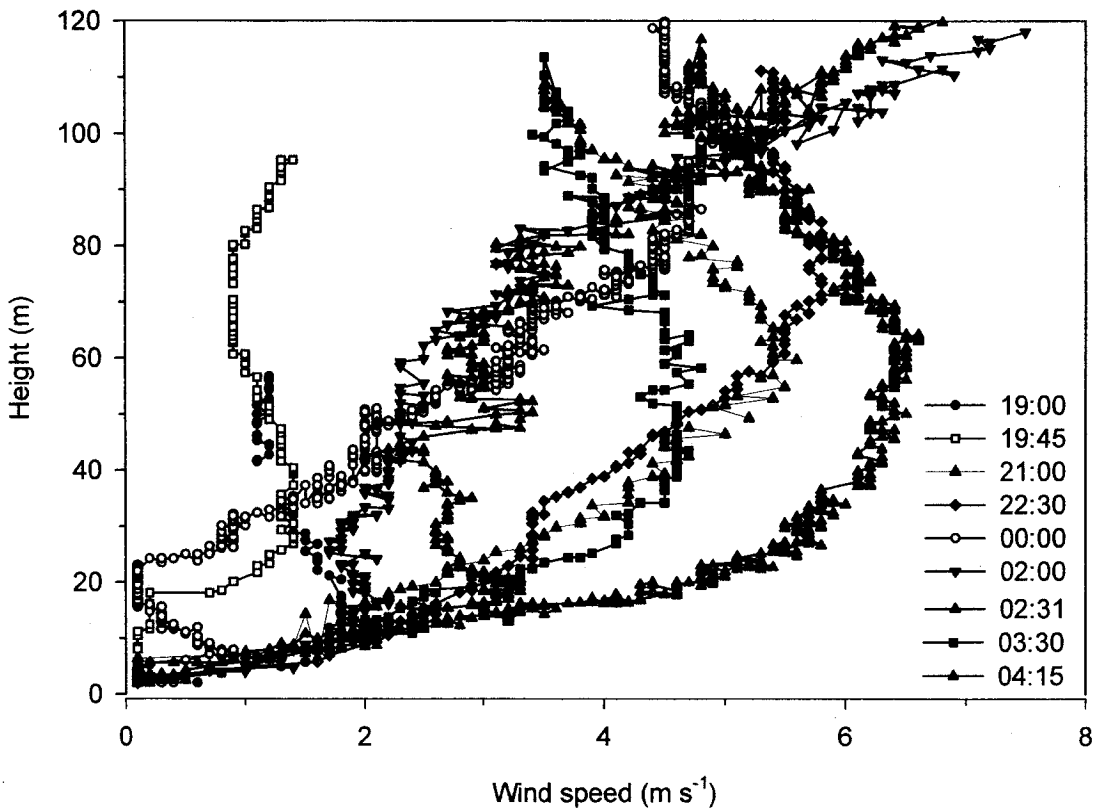

Figure 4.4 Wind speed profiles from tethersonde data for the 30-31 July, 2003. The wind speed maximum that had built up for the first part of the night, disappears around midnight as the perturbation occurs. The wind speed maximum re-develops following the wind shift.

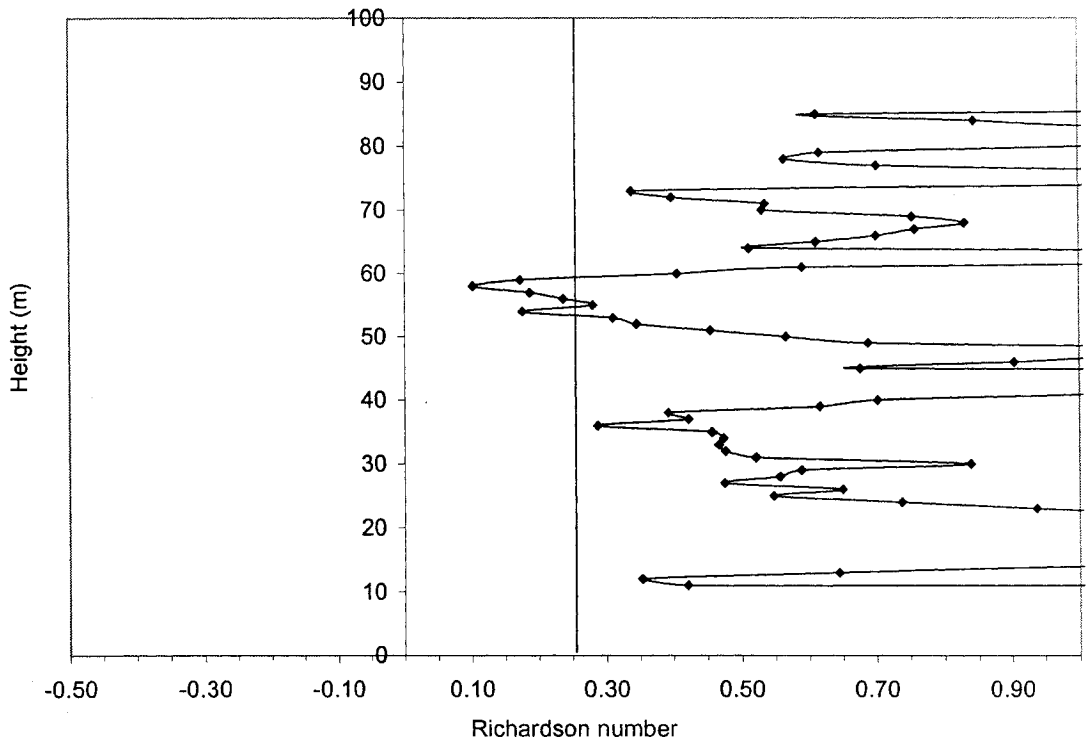

Figure 4.5 Profile of bulk Richardson number derived from tethersonde data at 00:00 EST for the 30-31 July, 2003. R_{iB} differentiates zones of stability from zones of potential turbulence. The majority of the profile is observed to be greater than the critical value of 0.25 (solid line) and therefore stable.

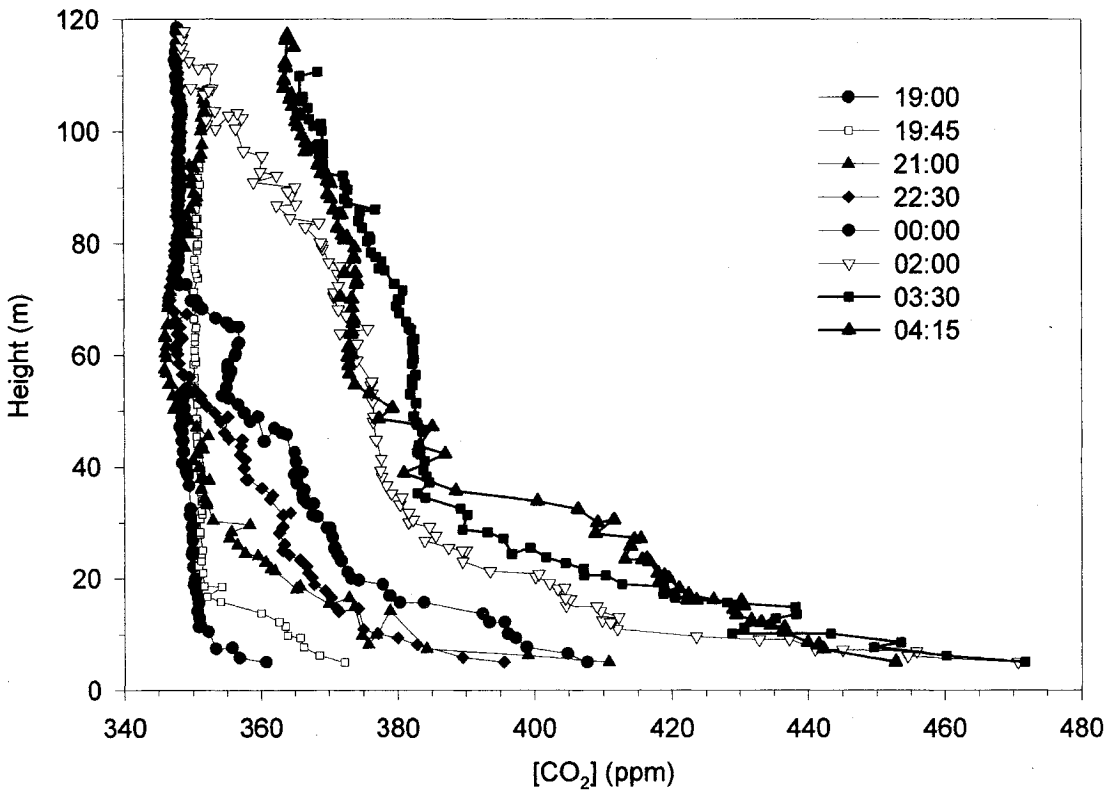

Figure 4.6 Profiles of CO_2 concentration throughout the night demonstrate the change in accumulation with time. Even though the length of time between ascents is not constant, the change between profiles 00:00 and 02:00 EST is clearly the largest of this night. A large increase at the ground as well as around 60 m can be seen and therefore a greater flux would be computed if this pair of profiles were used.

The increase between 60 and 80 m is substantial and again corresponds to the level at which descending motion was observed to increase.

4.3.2 Source of the anomaly

It is suggested here that the breakdown of the NBL was created by a density current that reached the ground bringing scalars from a distant and different source area. An examination of the wind direction measured by the tethersonde profiles provides the key. For the first part of the night (20:50 to 00:30), the wind originated from SE to SSE (130 -160°). The St. Lawrence River is situated in this exact direction in relation to the field site (see Figure 2.1b) at a distance of 2.65 km and 2.5 km, respectively for these wind directions. Following the disturbance, the wind direction shifted to the NEE to E (60 to 90°) or away from the river (Figure 4.7). Lapworth (2000) has reported the passage of a density current linked to the "sea breeze" type circulation where different scalars including temperature and gas concentration were transported.

Three wind shifts to the South in the profiles were observed: 19:45, 00:00 and 02:45. This wind shift was evident between 70 to 100 m at the first time, matching the interval which displayed large *w*. For the two other periods, the slight shift extends from 20 to 70 m and from 50m up, respectively. South is the most direct angle to the river and the disturbance could have originated from a circulation pattern created by the river. Lapworth (2000) also observed lower temperature induced by a sea breeze density current. This is believed to be the cause of the observed temperature drop at the ground as the density current brought down air that had been transported over several kilometres.

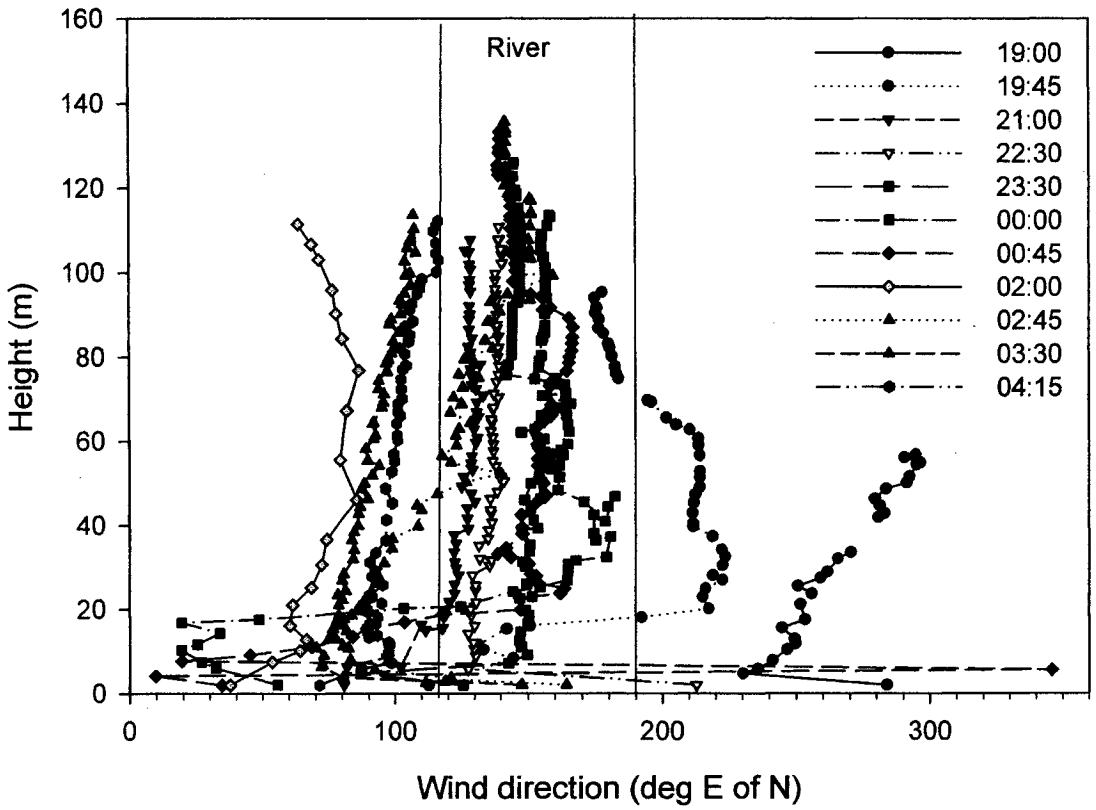

Figure 4.7 Wind direction profiles from tethersonde ascents. Wind direction is nearly consistent in originating from the direction of the St. Lawrence River (shown limited by the two solid lines) and then changes after the episode.

Additional evidence for this is found in the relative humidity profiles which also show changes corresponding to the passage of the event. Typically, during stable nights, relative humidity increases (often to 100%) as the temperature cools near the surface. During the night in question, the relative humidity was enhanced between the levels of interest (60 to 80 m) around the time of the breakdown (00:45 EST from Figure 4.8). This is consistent with a change in upwind source area towards a greater source of water vapour and cooler temperatures. A decrease in relative humidity at lower altitudes was observed after the passage of the event (2:45 EST) again suggesting the change in source area

4.3.3 Consequences of such events for the NBL technique

Waves in stable conditions transport scalars (Chimonas, 2002). On at least three separate nights, breakdowns of the NBL structure were observed that could have been due to wave propagation. In each of these nights, the redistribution of heat does not equal zero. There is an overall cooling of the layer which is not the result of either radiative cooling (as the measured net radiation was a constant negative flux for the entire nighttime period), or clear air radiative cooling (as this accounts for only a very small percentage of the gross radiative heat flux from the atmosphere at the Earth surface (Surridge, 1990)). Since the net transport is believed to add up to approximately zero when examining the transport of sensible heat over the whole NBL depth (Ohya and Uchida, 2003), we can conclude that some event brought a large mass of air through the NBL and was observed at our measurement location.

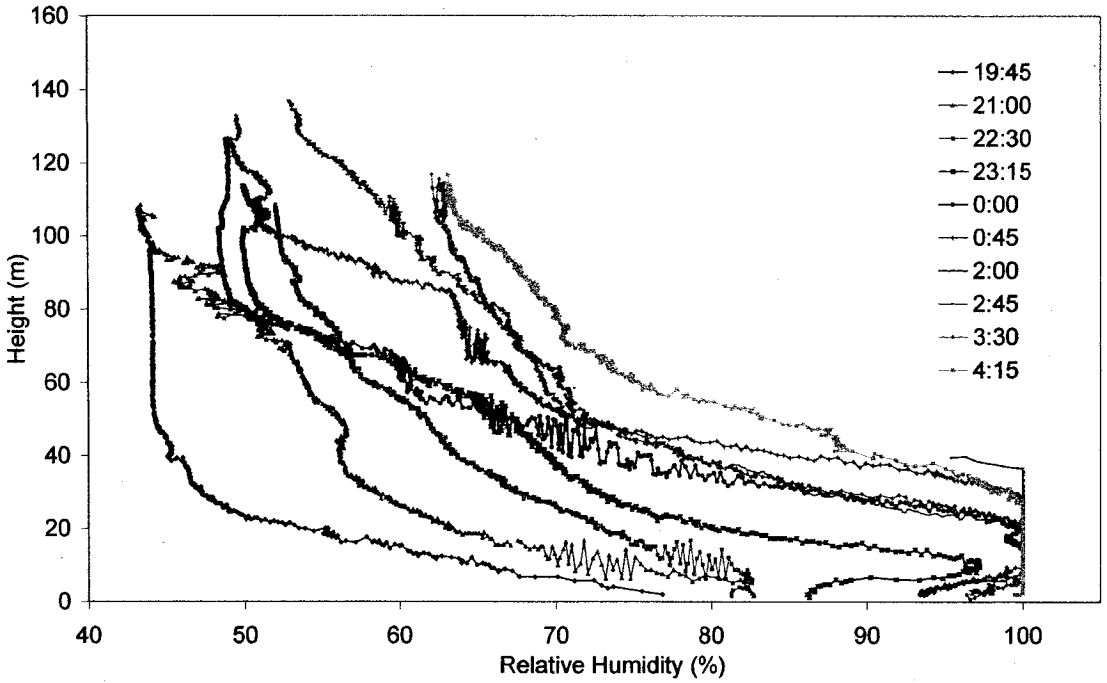

Figure 4.8 Profiles of relative humidity from tethersonde ascents. While most of the profiles of humidity increase throughout the night, there is a decline of humidity at lower heights after the passage of the event (02:45 EST). An important increase can also be seen between 60 and 80 m during the breakdown (00:45 EST).

In this case, it is suggested that a density current brought air with different CO_2 concentration, temperature and humidity characteristics through a distance before it was observed at the measurement site. Certainly, a change in the source area was observed during the event. A change in wind direction between profiles will result in different upwind source areas between the pairs of profiles. If these source areas have different characteristics (river dominated vs. agricultural land dominated) then, the calculated GHG flux does not represent the true accumulation from the agroecosystem over this time interval and therefore such event should be avoided when using the NBL budget technique.

4.4. Conclusion

Evidence of a strong and irregular event was investigated in light of the mini-SODAR trace of NBL height which suggested a complete breakdown in NBL structure mid-way through the night of July 30-31, 2003. Mini-SODAR estimates of w, tethersonde profiles of potential temperature and relative humidity and IRGA measurements of CO_2 each indicated separately, changes at specific heights within the NBL which culminated in the removal of the capping LLJ and changes to the accumulation of CO_2. The evidence suggested that a density current was the origin of the changes in the NBL structure, shifting the source area to the influence of the St. Lawrence River. These observations yield insights with respect to the extent of the source area, at the height at which this contribution is observed, and to what extent the flux calculated with the technique is affected.

Users of the NBL method as well as footprint modelers should be wary when interpreting data where a change in direction has occurred especially if a large body of water is involved in this direction change. Fluxes calculated with the NBL budget technique will contain large errors if such events are not taken into consideration.

Chapter 5. Conclusions and Scope for Future Study

5.1 Summary of findings

Although GHG measurement techniques are well-documented for daytime and windy nighttime conditions, an accurate estimate of nighttime GHG concentration is essential to complete the diurnal cycle. The nocturnal boundary layer (NBL) technique involves using the layer of the atmosphere closest to the ground as a giant measurement chamber. This technique has the advantage of using a layer which is large enough to include the spatial variability in emissions from the field (i.e. integrates hotspots). However, the chamber lid – a function of the stability of the nocturnal inversion - is not impermeable, turbulent intermittency could affect the gas distribution, and the upwind source are is difficult to define. A more robust utilization of the NBL technique requires knowledge of nighttime dynamics and associated vertical and horizontal gas propagation that are so important to account for in the flux calculation.

The results presented in Chapter 2 indicated that the low level jet was an important influence in terms of gas accumulation and was demonstrated to allow strong blockage of vertical gas propagation beneath the maximum wind speed, and rapid dispersion of gas in the upper portions. Since observations on multiple nights indicated gas accumulation that extended higher than the temperature inversion, it is suggested that the temperature inversion alone is not a good "lid" in all cases. The low level jet (LLJ) was found to be better at stopping vertical gas dispersion, but calculations using the NBL technique should never include measurements obtained from higher than this "lid". The more steady and close to the ground (while still remaining decoupled) the LLJ is, the lower the uncertainties surrounding the flux calculation will be.

The literature suggests that nighttime turbulence intermittency plays a major role in gas dispersion, but the investigation portrayed in Chapter 3 shows that, for the nights studied, this feature seemed to be less important than an observed slow vertical motion that maintains sign and strength with height, throughout the night. The potential influence of a systematic error through tilting of the sensor was investigated and rejected. It is proposed that the background motion is affecting accumulation by promoting vertical diffusion of gases. Nights with an overall ascending motion would lead to gas accumulation overshooting the stable layer resulting in greater gas leakage than when a well-defined cap exists to limit their vertical propagation. Intermittent turbulence observed by mini-SODAR was found to lie largely above a threshold of vertical wind speed of 0.2 ms^{-1} for the two full-nights nights studied resulting in 25% of the data classified as such. Of the two nights, the more stable night with a better defined jet was characterized by a higher number of intermittent events that had shorter duration and smaller vertical extent. It was found that all magnitudes of w contributed to the sign of the average vertical windspeed as there was a clear tendency for the vertical wind speed to maintain sign within a given night..

The new information provided in this thesis will assist in the classification of nights as being better suited for the development of a strong cap and reliable gas flux estimates. A better indication of the types of nights that are appropriate for the use of the NBL technique may be developed. The following classification is suggested:

1) Nights that are well-defined by a low turbulent height, h_R during constant LLJ events. These nights are expected to have low uncertainties associated with the calculated fluxes;

2) Nights that have no LLJ, but have a background descending motion. The NBL is observed to be well-defined under the inversion height, h_i. These nights are expected to contain acceptable uncertainty associated with the calculated fluxes;

3) Nights that have no LLJ and have a background ascending motion. These nights are expected to be prone to large uncertainties in the calculated fluxes.

The calculation of the upwind source area is also known to be problematic at night. No effective model of this exists and it is therefore difficult to determine the actual contribution of surface cover that is included in what is being measured. The results presented in Chapter 4 illustrate the importance of this knowledge as the influence of the St. Lawrence River was shown to affect measurements. An event, first observed as a strong descending motion, destroyed the NBL height around midnight of one of the nights of observation. A change in the humidity and potential temperature evolution at several heights, and the temporary disappearance of the LLJ followed from this event. Gas accumulation was also affected as the flux calculated for the period including the event was too large to be accounted by emissions alone. The cause of this event was likely indicated by the wind direction change towards and away from the river. It is suggested that a density current controlled by a land/see breeze and transporting scalars from a different source area was brought down to the ground at our measurement site. Certainly, users of the NBL technique need to consider the effects that changes in the upwind source area will have on the calculated fluxes.

5.2 Limitations and future considerations

There is a continued need for more information about the NBL (Galmarini *et al.*, 1998). This is especially true in the context of the current study where some interesting features of the nighttime atmosphere need to be investigated in greater detail. The mini-SODAR has proven to be an invaluable resource for the project, however, its availablilty was limited and additional data concurrent with balloon ascents is essential. It provides a method for better determination of NBL height, the presence of LLJ's and can be used to study atmospheric phenomenon like waves (Adedokun, 1997).

The potential temperature profile is an important factor influencing the vertical gas distribution. The temperature evolution can be an important indicator of events that disturb the gas concentration and therefore the flux measurements made with the NBL technique. For these reasons, measurements of the temperature profile between balloon ascents would be a powerful asset. Moreover, this feature would also permit the calculation of the Richardson number which is the best accepted measure of stability. Additionally, the Brünt Vaïsaïla frequency could be calculated and this could be used to study the existence of waves which are also an influential feature for gas displacement. The availability of a RASS system (for atmospheric temperature sounding) to the measurement package would therefore increase the scientific quality and improve the understanding of the features observed.

This thesis has focused on the vertical dispersion, however, it is also important to consider the horizontal dispersion. The extent of the footprint clearly needs to be better defined. To do so, two sets of balloon equipment should be deployed at different sides of the field to make concurrent measurements of gas concentrations as well as atmospheric

features. Differences in the measurements taken will provide a general idea of the impact of distance in the concentration collected as well as the importance of coverage of the source area. In addition, the coverage of specific atmospheric features that have a great impact on the technique, like the low level jet, will be evaluated. This technique has been attempted but the instrumentation and personnel costs are high (Strachan pers, comm.).

Having mainly considered the dispersion of gas using CO_2 concentration profiles, the next step would be to compare results with other gases of interest, namely methane and nitrous oxide. These gases are believed to act the same way with respect to atmospheric features, but mechanisms of emission are dissimilar and so the scale of emission may be different. Smaller fluxes may not react the same way to a disturbance. Events that were changing the carbon dioxide fluxes because they were bringing a different concentration from a different source area may not have the same impact on the flux calculated for other gases. For all those reasons, a detailed profile of all the gases in question is of major importance. This has been done in a limited number of studies (e.g., Pattey *et al.*, submitted).

References

Environment Canada: http://www.ec.gc.ca/climate/overview_what-e.html

Acedevo, O. C. and D. R. Fitzjarrald, 2003. In the Core of the Night –Effects of intermittent mixing on a horizontally heterogeneous surface, *Boundary-Layer Meteorology* 106:1-33

Adedokun, J.A., 1997. Sodar monitoring of nocturnal boundary layer during the harmattan in ile-ife, nigeria. In: S.P.Singal (Ed), *Acoustic Remote Sensing Applications*. Narosa Publishing House, New Delhi, India, pp.293-307.

Ahrens, C. D., 1994. Meterology Today: An introduction to weather, climate, and the environment, fifth edition. West Publishing Company, pp 68-70.

Alcamo, J. and R. Swart, 1998. Future trends of land-use emissions of major greenhouse gases. *Mitigation and adaptation Strategies for Global Change* 3:343-381

Anderson, C. J. and R. W. Arritt, 2002. Representation of summertime low-level jets in the central united states by the ncep-ncar reanalysis. *Journal of Climate* 14:234-247

André, J.C. and L. Mahrt, 1982. The nocturnal surface inversion and iinfluence of clear-air radiative cooling. *Journal of the Atmospheric Sciences* 39: 864-877

Andreas, E.L., Claffey, K.J. and A.P. Makshtas, 2000. Low-level atmospheric jets and inversions over the western weddell sea. *Boundary-Layer Meteorology* 97:459-486.

Arrhenius, S.,1896. On the influence of carbonic acid in the air upon the temperature of the ground. *Phil. Mag. Sci.* 5:237-276.

Baldocchi, D.,2003. Assessing the eddy covariance technique for evaluating carbon dioxide exchange rates of ecosystems: past, present and future. *Global Change Biol.* 9:479–492.

Bange, J. and R. Roth, 1999. Helicopter-borne flux measurements in the nocturnal boundary layer over land- a case study. *Boundary-Layer Meteorology*, 92:295-325.

Banta, R.M., Newsom, R.K., Lundquist, J.K., Pichugina, Y.L., Coulter, R.L. and L. Mahrt, 2002. Nocturnal low-level jet characteristics over kansas during CASES-9. *Boundary-Layer Meteorology,* 105:221-252.

Beyrich, F., Kalass, D. and U. Weisensee, 1997. Influence of the nocturnal low-level-jet on the vertical and mesoscale structure of the stable boundary layer as revealed from doppler-sodar-observations. In: S.P. Singal (Ed.), *Acoustic Remote Sensing Applications*, Narosa Publishing House, New Delhi, India, pp.236-246.

Beyrich, F., 1994. Sodar observations of the stable boundary layer height in relation to the nocturnal jet. *Meteorol. Zeitschrift,* 3:29–34.

Beyrich, F. and A. Weill, 1993. Some aspects of determining the stable boundary layer depth from sodar data. *Boundary-Layer Meteorology.*, 63:97–116.

Blackadar, A.K., 1957. Boundary layer maxima and their significance for the growth of nocturnal inversions. *Bulletin of the American Meteorological Society,* 38:283-290.

Brost R. A. and J. C. Wyngaard, 1978. A model study of the stably stratified planetary Boundary Layer. *Journal of the Atmospheric Sciences,* 35:1427-1440.

Bull, G., 1997. Some investigations of gravity waves by cross spectral analysis. In: S.P. Singal (Ed.), *Acoustic Remote Sensing Applications*, Narosa Publishing House, New Delhi, India, pp.275-292.

Businger, J.A., 1986. Evaluation of the accuracy with which dry deposition can be measured with current micrometeorological techniques. *Journal of Climate and Applied Meteorology,* 25:1100–1124.

Carslaw, D. C. and S. D. Beevers, 2002. Dispersion modelling considerations for transient emissions from elevated point sources. *Atmospheric Environment* 36:3021-3029.

Carlson, M. A.and R. Stull, 1986. Subsidence in the nocturnal boundary layer. *Journal of Climate and Applied Meteorology* 25:1088-1099.

Chatterjee, K. and S. Huq, 2002. A report the inter-regional conference on adaptation to climate change. *Mitigation and Adaptation Strategies for Global Change* 7:403-406.

Cheung, T.K. and C.G. Little, 1990. Meteorological tower, microbarograph array, and sodar observations of solitary-like waves in the nocturnal boundary layer. *Journal of the Atmospheric Sciences*, 47 (21):2516-2536.

Chimonas, G., 2002. On internal gravity waves associated with the stable boundary layer. *Boundary-Layer Meteorology*, 102:139-155.

Chimonas, G., 1999. Steps, waves and turbulence in the stably stratified planetary Boundary Layer. *Boundary-Layer Meteorology*, 90:397-421.

Corsmeier, U., Kalthoff, N., Kolle, O., Kotzian, M. and F. Fiedler, 1997. Ozone concentration jump in the stable nocturnal boundary layer during a llj-event. *Atmospheric Environment*, 31 (13):1977-1989.

Coulter, R.L. and J. C. Doran, 2002. Spatial and temporal occurrences of intermittent turbulence during CASES-99. *Boundary-Layer Meteorology*, 105:329-349.

Coulter, R.L., 1997. Turbulence variables derived from sodar data. In: S.P.Singal (Ed), *Acoustic Remote Sensing Applications*, Narosa Publishing House, New Delhi, India, pp.191-201.

Denmead, O.T., Leuning, R., Griffith, D.W.T. and C.P. Meyer, 1999. Some recent developments in trace gas flux measurement techniques, In: A.F. Bouwman, *Approaches to scaling a trace gas fluxes in ecosystems*, Elsevier Science B.V. pp 69-84.

Denmead, O.T., Raupach, M.R., Dunin, F.X., Cleugh, H.A. and R. Leuning, 1996. Boundary layer budget for regional estimates of scalar fluxes. *Global Change Biology* 2:255-264.

Derbyshire, S. H., 1999. Stable boundary-layer modelling: established approaches and beyond. *Boundary-Layer Meteorology* 90:423-446.

Edwards, G.C., Neumann, H.H., den Hartog, G., Thurtell, G.W. and G.Kidd, 1994. Eddy correlation measurements of methane fluxes using a tunable diode laser at the kinosheo lake tower site during the northern wetlands study (NOWES). *Journal of Geophysical Research*, 99:1511–1517.

Edwards, G.C., Thurtell, G.W., Kidd, G.E., Dias, G.M. and C. Wagner-Riddle, 2003. A diode laser based gas monitor suitable for measurement of trace gas exchange using micrometeorological techniques. *Agricultural and Forest Meteorology*, 115:71–89.

Engelbart, D. A. M. and J. Bange, 2002. Determination of boundary-layer parameters using wind profiler/RASS and SODAR/RASS in the frame of the LITFASS project. *Theoretical and Applied Climatology*, 73:53-65.

Etling, D., 1990. On plume meandering under stable stratification. *Atmospheric Environment* 24A (8):1979-1985.

Finn, D., Lamb, B., Leclerc, M.Y. and T. W. Horst, 1996. Experimental evaluation of analytical and lagrangian surface-layer flux footprint models. *Boundary-Layer Meteorology* 80:283-308.

Fitzjarrald D. R. and K. E. Moore, 1990. Mechanisms of nocturnal exchange between the rain forest and the atmosphere. *Journal of Geophysical Research*, 95d:16,839-16,850.

Foken, T. and M. Y. Leclerc. Methods and limitations in validation of footprint models. Special Issue: 'Footprint of Fluxes and Concentrations', *Agricultural and Forest Meteorology*, In press.

Fowler, D., Hargreaves, K. J., Skiba, U., Milne, R., Zahniser, M. S., Moncrieff, V, Beverland, V and M. W. Gallagher, 1995. Measurements of CH4 and N2O fluxes at the landscape scale using micrometeorological methods. *Philosophical Transactions of the Royal Society of London*, B 351:339-356.

Galmarini, S., Beets, C., Duynkerke, P.G. and J. Vilà-Guerau De Arellano, 1998. Stable nocturnal boundary layers: a comparison of one-dimensional and large-eddy simulation models. *Boundary-Layer Meteorology*, 88: 181-210.

Garratt, J. R. and R.A. Brost, 1981. Radiative cooling effects within and above the nocturnal boundary layer. *Journal of the Atmospheric Sciences*, 38:2730-2746.

Gopalakrishnan, S.G.and M. Sharan, 1998. Study of radiative and turbulent processes in the stable boundary layer under weak wind conditions. *Journal of the Atmospheric Sciences*, 55:954- 960.

Griffith D.W.T., Leuning, R., Denmead O.T.and I.M. Jamie, 2002. Air-land exchanges of co_2, ch_4 and n_2o measured by ftir spectrometry and micrometeorological techniques. *Atmospheric Environment*, 36:1833-1842.

Ha, K.-J. and L. Mahrt, 2001. Simple inclusion of z-less turbulence within and above the modeled nocturnal boundary layer. *Monthly Weather Review*, 129:2136-2143.

Hastie, D. R., Shepson, P.B., Sharma, S. and H. I. Schiff, 1993. The influence of the nocturnal boundary layer on secondary trace species in the atmosphere at dorset, Ontario. *Atmospheric Environment*, 27A (4):533-541.

Hénault. C., Devis, X., Lucas, J.L. and J.C. Germon, 1998. Influence of different agricultural practices (type of crop, form of N-fertilizer) on soil nitrous oxide emissions. *Biol. Fertil. Soils,* 27:299–306.

Hoffert, M. I., Caldeira, K. Benford, G., Criswell, D. R., Green, C., Herzog, H., Jain, A. K., Kheshgi, H. S., Lackner, K. S., Lewis, J. S., Lightfoot, H. D., Manheimer, W., Mankins, J. C., Mauel, M. E., Perkins, L. J., Schlesinger, M. E., Volk, T. and T. M. L. Wigley, 2002. Advanced technology paths to global climate stability: energy for a greenhouse planet. *Science*, 298:981-987.

Hollinger, D. Y., Kelliher, F. M., Byers, J. N., Hunt, J. E., McSeveny, T. M. and P. L. Weir, 1994. Carbon dioxide exchange between an undisturbed old-growth temperate forest and the atmosphere. *Ecology*, 75:134-150

Kallistratova, M.A, 1997. Physical grounds for acoustic remote sensing of the atmospheric boundary layer. In: S.P. Singal (Ed), *Acoustic Remote Sensing Applications*. Narosa Publishing House, New Delhi, India, pp.3-34.

Kormann, R. and F. X. Meixner, 2001. An analytical footprint model for non-neutral stratification. *Boundary-Layer Meteorology*, 99:207-224.

Kulshreshtha, S. N., Junkins, B. and R. Desjardins, 2000. Prioritizing greenhouse gas emission mitigation measures for agriculture. *Agricultural Systems*, 66:145-166.

Lapworth, A., 2000. Observations of atmospheric density currents using a tethered balloon-borne turbulence probe system. *Quarterly Journal of the Royal Meteorology Society*, 126:2811-2850.

Laville, P., Jambert, C., Cellier, P. and R. Delmas, 1999. Nitrous oxide fluxes from a fertilised maize crop using micrometeorological and chamber methods. *Agricultural and Forest Meteorology*, 96:19-38.

Leclerc, M. Y. and G. W. Thurtell, 1990. Footprint prediction of scalar fluxes using a markovian analysis. *Boundary-Layer Meteorology,* 52:247-258.

Lee, X., Neumann, H. H., Denhartog, G., Fuentes, J.D., Black, T.A., Mickle, R.E., Yang, P. C. and P.D. Blanken, 1997: observation of gravity waves in a boreal forest. *Boundary-Layer Meteorology,* 84:383-398.

Leuning, R., Raupach, M.R., Coppin, P.A., Cleugh, H.A., Isaac, P., Denmead, O.T., Dunn, F. X., Zegelin, S. and J. Hacker, 2004. Spatial and temporal variations in fluxes of energy, water vapour and carbon dioxide during oasis 1994 and 1995. *Boundary-Layer Meteorology,* 110:3-38.

Mahrt, L., Sun, J., Blumen, W., Delany, T. ND and S. Oncley, 1998. Nocturnal boundary-layer regimes. *Boundary-Layer Meteorology*, 88:255-278.

Mahrt, L., 1999. Stratified atmospheric boundary layers. *Boundary-Layer Meteorology* 90:375-396.

Mahrt, L, 1989. Intermittency of atmospheric turbulence. *Journal of the Atmospheric Sciences*, 46:79-95.

Mahrt, L. and N. Gamage, 1987. Observations of turbulence in stratified flow. *Journal of the Atmospheric Sciences*, 44:1106-1121.

Mahrt, L., 1985. Vertical structure and turbulence in the very stable boundary layer. *Journal of the Atmospheric Sciences*, 42:2333-2349.

Mazzeo, N. A. and L.E. Venegas, 1991. Air pollution model for an urban area. *Atmospheric Ressearch*. 26:165-179.

Meyer, C. P., Galbally, L.E., Wang, Y.-P., Weeks, I. A., Jamie, I. and D.W.T. Griffith, 2001. Two automatic chamber techniques for measuring soil-atmosphere exchanges of trace gases and results of their use in the OASIS field experiment. *CSIRO Atmospheric Research Technical Paper*, 51, CSIRO, Melbourne

Moncrieff, J.B., Malhi, Y. and R. Leuning, 1996. The propagation of errors in long-term measurements of land-atmosphere fluxes of carbon and water. *Global Change Biology,* 2:231-240.

Mylne, K. R., 1992. Concentration fluctuation measurements in a plume dispersing in a stable surface layer. *Boundary-Layer Meteorology*, 60:15-48.

Nappo, Carmen J., 1991. Sporadic breakdowns of stability in the PBL over simple and complex terrain. *Boundary-Layer Meteorology* 54:69-87.

Nieuwstadt, F. T. M. and H. Tennekes, 1980. A rate equation for the nocturnal boundary layer height. *Journal of the Atmospheric Sciences,* 38:1418-1428.

Nieuwstadt, F.T.M., A.G.M. Driedonks, 1979. The nocturnal boundary layer-a case study compared with model calculations. *Journal of Applied Meteorology,* 18:1397-1405.

Ohba, R., Ukeguchi, N., Kashima, S. and B. Lamb, 1990. Wind tunnel experiment of gas diffusion in stably stratified flow over a complex terrain. *Atmospheric Environment,* 24A (8):1987-2001.

Ohya, Y. and T. Uchida, 2003. Turbulence structure of stable boundary layers with a near-linear temperature profile. *Boundary-Layer Meteorology,* 108:19-38.

Olsen, K., Wellish, M., Boileau, P., Blain, D., Ha, C., Henderson, L., Liang, C., McCarthy, J. and S. McKibbon, 2003. Canada's greenhouse gas inventory: 1990-2001. Environment Canada, Greenhouse Gas Division, Ottawa

Pattey, E., Strachan, I. B., Desjardins, R. L., Zhu, T., Dow, D. and I. MacPherson. CH_4 and N_2O fluxes measured using various micrometeorological techniques. In press.

Pattey, E., Strachan, I.B., Desjardins, R.L. and J. Massheder, 2002. measuring nighttime co2 flux over terrestrial ecosystems using eddy covariance and nocturnal boundary layer methods. *Agricultural and Forest Meteorology*, 113:145-158.

Piomelli, U., 1999. large-eddy simulation: achievements and challenges. *Progress in Aerospace Sciences,* 35:335-362.

Pleune, R., 1990. Vertical diffusion in the stable atmosphere. *Atmospheric Environment,* 24A (10):2547-2555.

Poulos, G. S., Blumen, W., Fritts, D. C., Lundquist, J. K, Sun, .J., Burns, S. P., Nappo, C., Banta, R., Newsom, R., Cuxart, J., Terradellas, E., Basley, B. and M. Jensen, 2002. Cases-99: a comprehensive investigation of the stable nocturnal boundary layer. *Bulletin of the American Meteorological Society*, 60:555-581.

Rees, J. M., Anderson, P.S., and J.C. King, 1998. Observations of solitary waves in the stable atmospheric boundary layer. *Boundary-Layer Meteorology*, 86:47-61.

Rochette, P., Ellert, B., Gregorich, E. G., Desjardins, R. L., Pattey, E., Lessard, R. and B. G. Johnson, 1997. Description of a dynamic closed chamber for measuring soil respiration and its comparison with other techniques. *Canadian Journal of Soil Science*, 77:195-203.

Saiki, E. M., Moeng, C.-H. and P.P. Sullivan, 2000. Large-eddy simulation of the stably stratified planetary boundary layer. *Boundary-Layer Meteorology,* 95:1-30.

Schmid, H.P., 1994, Source areas for scalars and scalar fluxes. *Boundary-Layer Meteorology,* 67:293-318.

Schuepp, P.H., Leclerc, M.Y., Macpherson, J.I. and R.L. Desjardins, 1990. Footprint prediction of scalar fluxes from analytical solutions of the diffusion equation. *Boundary-Layer Meteorology*, 50:355-373.

Singal, S. P., 1989. Acoustic sounding stability studies. *Encyclopedia of Environmental Control Technology,,* P. N. Cheremisinoff, Ed., 2, Gulf, pp. 1003–1061

Smedman, A.-S., 1988. Observations of a multi-level turbulence structure in a very stable atmospheric boundary layer. *Boundary-Layer Meteorology,* 44:247–264.

Sorbjan, Z. and Uliasz, M., 1999. Large-eddy simulation of air pollution dispersion in the nocturnal cloud-topped atmospheric boundary layer. *Boundary-Layer Meteorology*, 91:145-157.

Stull, R. B.,1988. An introduction to boundary layer meteorology. Kluwer Academic Publishers, Dordrecht, 666p.

Stull, R. B., 1983. Integral scales for the nocturnal boundary layer. part 2: heat budget, transport and energy implications. *Journal of Climate and Applied Meteorology*, 22:1932-1941.

Sun, J., Lenschow, D. H., Burns, S. P., Banta, R. M., Newsom, R. K., Coulter, R., Frasier, S., Ince, T., Nappo, C., Balsey, B. B., Jensen, M., Mahrt, L., Miller, D. and B. Skelly: 2004. Atmospheric disturbances that generate intermittent turbulence in nocturnal boundary layers. *Boundary-Layer Meteorol.* 110:255-274.

Surridge, A. D., 1990. The stable boundary layer temperature profile and the effect of heat loss from the body of the atmosphere. *Atmospheric Environment* 24A (5):1285-1296.

Surridge A. D. and D. J. Swanepoel, 1987. On the evolution of the height and temperature difference across the nocturnal stable boundary layer *Boundary-Layer Meteorology,* 40:87-98.

Tuhkanen, S., Savolainen, A. and I. Savolainen, 1999. The role of CH_4 and N_2O emissions in the cost-effective control of the greenhouse gas emissions from Finland. *Mitigation and Adaptation Strategies for Global Change,* 4:91-111.

Van de Wiel, B. J. H., Moene, A. F., Ronda, R. J., De Bruin, H. A. R. and A. A. M. Holtslag, 2002a. Intermittent turbulence and oscillations in the stable boundary layer over land, part 1: a bulk model. *Journal of the Atmospheric Sciences,* 59:942-958.

Van de Wiel, B. J. H., Moene, A. F., Ronda, R. J., De Bruin, H. A. R. and A. A. M. Holtslag, 2002b. Intermittent turbulence and oscillations in the stable boundary layer over land, part 2: a system dynamics approach. *Journal of the Atmospheric Sciences,* 59:2567-2581.

Van de Wiel, B. J. H., Moene , A. F., Hartogensis, O.K., De Bruin, H. A. R. and A. A. M. Holstag, 2003. Intermittent turbulence and oscillations in the stable boundary layer over land, part 3: a classification for observations during CASES-99. *Journal of the Atmospheric Sciences,* 60:2509-2522.

Wagner-Riddle, C., Thurtell, G.W., King, K.M., Kidd, G.E. and E.G. Beauchamp,1996a. Nitrous oxide and carbon dioxide fluxes from a bare soil using a micrometeorological approach. *Journal of Environmental Quality,* 25:898–907.

Wagner-Riddle, C., Thurtell, G.W., Kidd, G.E., Edwards, G.C. and I.J. Simpson, 1996b. micrometerological measurements of trace gas fluxes from agricultural and natural ecosystems, *Infr. Phys. Tech.,* 37:51–58.

UNFCCC, 1997. kyoto protocol to the united nations framework convention on climate change. UNFCCC Secretariat, Bonn, FRG

Zhou, M., 1997. Development of sodar detection and its application for studies of atmospheric boundary layer in Beijing, China. In: *Acoustic Remote Sensing Applications*, S.P. Singal (Ed), Narosa Publishing House, New Delhi, India, pp.

Appendix A

Meteorological conditions of the complete nights						
	JUNE 28-29, 2002	JULY 18-19, 2002	JUNE 16-17, 2003	JUNE 20-21, 2003	JULY 9-10, 2003	JULY 30-31, 2003
Average Pressure (kPa)	100.5	100.5	101.9	101.1	101.4	101.8
change in pressure (kPa)	0	0	-0.1	0.1	0.5	0.02
Average surface wind speed (ms^{-1})	0.9	0.78	0.48	0.50	0.98	0.69
Maximum temperature inversion strength (°C)	>10.5	>5.9	>7.3	>9.2	9.2	>9.7
Rate of potential temperature evolution ($°Ch^{-1}$)	-0.83	-1.15	-0.85	-0.74	until 2h30: -0.90 after: 0.87	until 23h30: -1.00 after: 0
Approximate NBL depth (temperature inversion) (m)	100	100	140	120	60	100
CO_2 accumulation overshooting temperature inversion	mostly no because of LLJ	mostly yes	mostly no	mostly no	yes	mostly no
Maximum wind speed observed (ms^{-1})	7	no wind maximum in profiles	4.5	4	8	6.5
Figure references	2.1a, 2.2a, 2.3, 2.5, 2.6, 2.7, Table 2.1			2.4		2.1b, 2.2b, 2.8, 2.9, 2.10, Table 2.1

The different meteorological data measured for complete nights of observation. Pressure, surface wind, temperature and pressure change were taken from a meteorological instrument tower at a height of 6 m above the ground surface. The temperature inversion strength, the depth of the NBL (inversion height) and maximum wind speed observed were extrapolated from the multiple tethersonde ascent data taken for each night. "CO_2 accumulation overshooting the NBL depth" occurred for profiles where the concentration didn't return to the concentration of the previous profile.